NTNU

Norwegian University of
Science and Technology

Fault Ride Through Capability Analysis of Small-Scale Hydro Power Plants

Kristine Mamen Antonsen

Master of Energy and Environmental Engineering
Submission date: June 2016
Supervisor: Trond Toftevaag, ELKRAFT
Co-supervisor: Henrik Kirkeby, SINTEF Energi

Norwegian University of Science and Technology
Department of Electric Power Engineering

Problem Description

Fault ride through capability[1] requirements found in various grid codes are related to characteristics which depict voltage magnitude in relation to time. Realistic faults will not only change the magnitude, but also the angle of the voltage. This study will comprise analysis of the following:

- Characteristics of transient faults, based on an introductory survey of statistical information (type of fault and voltage magnitude).
- Impact of voltage angle in the fault ride through capability assessment.

An evaluation of the current requirements given in the grid codes based on the above work, simulations and in-field testing will be made.

SINTEF Energy Research have during spring 2016 use the DipLab to test the FRT capability on a small hydro power plant. A model validation will be performed in this context, based on measurement results.

If time permits, also in-house lab experiments will be performed, as a basis for model validation and further analysis.

1. Low voltage ride through

Preface and Acknowledgements

This master thesis is written in the spring semester 2016. The report is the final work of the 5-year master program Energy and Environmental Engineering at Norwegian University of Science and Technology (NTNU). The report is written at the Department of Electrical Power Engineering. This master thesis is a continuation of the specialization project carried out in the autumn semester 2015, and study the fault ride through capability assessment of distributed generating units. Data simulations have been compared to laboratory experiment results, and the impact of voltage angle in the critical clearing time of a synchronous generator connected to the distribution grid have been studied.

I would like to express my gratitude to my co-supervisor Henrik Kirkeby in SINTEF Energy Research for the opportunity to take part in the SINTEF Dip Test project. It has been interesting to be able to study a full size power plant, and to be a part of the tests made at Bruvollelva in April 2016. I will also thank for great help and guidance regarding both laboratory work and the final report.

I am also thankful for the help from Bård Almås, Svein Erling Norum and Aksel Hanssen at the Service Lab for the help during the construction and execution of the in-house lab.

Last, but not least, I would like to thank my supervisor Trond Toftevaag for valuable help.

Trondheim, June 2016
Kristine Mamen Antonsen

Abstract

This master thesis has looked upon the fault ride through capability assessment for small-scale hydro power plants in the distribution grid. In this report, the shape of the voltage dip has been studied, and the voltage angle impact on critical clearing time has been analysed. A model of the Snåsa grid has been used to study faults with the simulation program SIMPOW. The SINTEF DipLab has been simulated, and the results from simulations have been compared to measurements made during experiments at Bruvollelva power plant. An in-house lab has been built to study the significance of the surrounding grid, as a weaker grid connection theoretically increases the voltage angle fluctuations, and hence decreases the critical clearing time of the generator.

When studying the voltage dips caused by three phase symmetrical faults in the distribution grid, the location of the fault has proven to be important. One of the reasons is the difference in voltage angle. The voltage dips with origin in a fault in a parallel radial to the point of measurement gives a small fluctuation in voltage angle, while faults between the point of measurement and the swing bus creates larger changes in voltage angle. The reason is that the whole load flow changes when the swing bus is disconnected, and the DG units have to cover all the demand.

The critical clearing time for the distributed generating unit Bruvollelva was simulated in this report for two different cases. A symmetrical fault was implemented, and the same voltage profile was then implemented without the same voltage angle response. The increase in critical clearing time was about 20% for the voltage dips with origin between the DG unit and the swing bus, while the increase was much lower for the faults with origin in a parallel radial. A correlation can be seen, as the faults leading to the highest fluctuations in voltage angle was the same faults that gave the largest increases in clearing time. This indicates that the voltage angle has a considerable impact on the critical clearing times of the machine, and hence a considerable impact on the fault ride through capability assessment. The implementation guidelines for network codes amplifies the importance of the short-circuit capacity at the connection point in the pre-fault and post-fault condition. The robustness of the network has significant impact of the FRT performance, and a minimum requirement for short circuit capacity should be defined in the national FRT restrictions.

An in-house lab was built to verify the results from the simulations. The outcome was surprising, as a weak grid connection lead to a clearing time of 600 ms when the generator was operating at 7 Nm, while the stronger grid connection made the generator trip at 500

ms. The experiments should however have been made with a longer cable, and should be repeated to increase the credibility of the results.

Another verification of the simulation model was made when the measurements from the experiments made at Bruvollelva was compared to simulations. The results showed that the voltage dips were similar. Protection relays should also have been implemented to the simulations model, as they were a limiting factor when it came to the clearing time of the fault.

Generally, the measured dips caused by the DipLab were more square shaped than the simulated dips. It has been showed that the voltage due to a three phase fault is less square shaped at the generator nodes than in the rest of the system due to a higher inductance in the short circuit impedance. This is especially the case for periods with high production.

Sammendrag

I denne masteroppgaven har FRT-kravene til småkraftverk i det norske distribusjonsnettet blitt vurdert. Kravene er i dag uttrykket ved en firkantet spenningsdipp, der amplituden til spenningen blir gitt som en funksjon av tiden. I denne rapporten har fasongen til spenningskurven blitt vurdert opp mot realistiske feil, og spenningsvinkelens betydning for generatorens kritiske klareringstid har blitt studert.

En modell av Snåsanettet er laget i simuleringsverktøyet SIMPOW. SINTEFs DipLab has også blitt implementert i simuleringsmodellen, og resultatene har blitt sammenlignet med faktiske målinger gjennomført på Bruvollelva kraftverk i april 2016. En mini-versjon av DipLaben ble laget innendørs for testing av en 1 kW labmaskin. Målet var å studere betydningen av styrken på nettilkoblingen, og dermed se i hvilken grad spenningsvinkelen faktisk har betydning for generatorens kritiske klareringstid.

Hvor i nettet en feil oppstår har vist seg å spille en betydelig rolle i studiet av transiente forstyrrelser. Kortslutninger som skiller målepunktet fra det stive nettet, og dermed skaper en midlertidig øydrift gir store svingninger i spenningsvinkel, mens kortslutninger som skjer i en parallell radial slik at den stive nettet fortsatt er koblet til målepunktet påvirker både lastflyten og spenningsvinkelen i mye mindre grad.

Den maksimale varigheten til en forstyrrelse før generatoren mister synkronisme er simulert for to ulike tilfeller i modellen av Snåsanettet. Først ble symmetrisk feil implementert på en node i systemet, og den kritiske klareringstiden til generatoren ble funnet. Videre ble den samme spenningsdippen påtrykket på generatorterminalene, men uten at spenningsvinkelen ble påvirket i særlig grad. En økning i kritisk klareringstid på 20% ble vist for feil mellom målepunktet og det stive nettet, mens økningen var liten i tilfellene der feilen skjedde i en parallell gren. En sammenheng kan bli sett, da forstyrrelsene som ga store endringer i spenningsvinkel også var de som hadde store økninger i kritisk klareringstid. Den tydelige korrelasjonen indikerer dermed at spenningsvinkelen har en betydelig påvirkning på klareringstiden, og burde tas hensyn til i utviklingen av FRT-krav.

Allerede er kortslutningsytelsen nevnt i et dokument der retningslinjer for implementering av FRT-krav er gitt. Nettets robusthet har stor betydning for evnen til å fortsette med en synkron produksjon også etter transiente feil, og en minimum kortslutningsytelse i nettet burde derfor være gitt for at krav skal kunne settes til de tilknyttede kraftverkene.

For å verifisere resultatene fra simuleringene ble en innendørs lab satt opp. En spenningsdipp ble laget ved hjelp av en kortslutningsreaktans og en bryter med samme prinsipp

som i DipLaben. Den kritiske klareringstiden ble funnet, og en lang kabel ble så koblet mellom testobjektet og nettet for å gjøre tilkoblingen svakere, og svingningene i spenningsvinkel større. Resultatene var overraskende, da klareringstiden gikk fra 500 til 600 ms da kabelen ble koblet inn. Eksperimentet skulle dog ha blitt gjennomført med flere repetisjoner for mer pålitelige resultater.

En verifisering av simuleringsmodellen ble også gjort da målte resultater fra DipLab-prosjektet ble sammenlignet med simuleringer. Generelt var det godt samsvar mellom de to, men vern skulle ha vært implementert i simuleringsmodellen, da dette viste seg å være avgjørende for kraftverkets FRT-egenskaper.

En generell observasjon gjort i denne oppgaven var at de målte spenningsdippene var mer firkantede enn de simulerte. Det har blitt vist at spenningsdippene ved en generator er mindre firkantede enn i resten av nettet, da kortslutningsimpedansen vil ha en betydelig reaktiv komponent. Dette er spesielt tilfelle i perioder med stor produksjon.

Table of Contents

List of Tables

List of Figures

1 | Introduction

Distributed generation (DG) is often renewable, and is based on sources such as run of river hydro, wind and solar. All the sources mentioned are intermittent by nature, which makes it difficult for the grid operator to predict and control. As more power from renewable energy sources cover the energy mix i Europe, a new set of rules must be made to ensure a stable electricity system in the future with a stable and reliable grid operation.

Network codes elaborated by the European Network of Transmission System Operators (ENTSO-E) are made to secure products necessary for an efficient pan-European market in generator technology. The Fault Ride Through (FRT) Capability in small power plants is one of the topics in the new network codes. The FRT requirements are related to a voltage profile, for which the generating unit are required to stay connected to the grid after the clearing of the fault. The FRT restrictions concern the magnitude of the voltage, and voltage phase angle are not of concern. This report is based on the project thesis "Low voltage Fault ride through capability in mini-hydro power plants - modelling and simulations of Bruvollelva kraftverk"[2], where the FRT capability in an already existing plant was simulated. A model of the SINTEF DipLab was also implemented to see to what extent the lab could be used to find the FRT curve for the power plant. The results was compared to the curves found in grid codes.

In this report, the critical clearing time have been simulated during realistic faults and for a system where the power plant experienced a voltage dip where only the voltage magnitude was changed. The results from the experiments made with the DipLab at Bruvollelva power plant will be presented, and compared to computer simulations. An in-house small scale DipLab has been made, to look into the FRT capability of a 1 kW synchronous generator connected to a strong grid and to a weaker grid.

1.1 Objectives

The objective of this report is to evaluate the proposed network codes. The importance of including the voltage angle in the assessment will be studied, and the coherence between simulations and measurements will be seen.

1.2 Scope of Work

The work comprises the following:

- A literature study covering subjects such as FRT restrictions, transient rotor angle stability, generating unit control systems and a short study of the characteristics of typical transient faults in the Norwegian power grid, looking at types of faults and the shapes of the voltage dips.
- An introduction to the models used for computer simulations, including a presentation of the parameters used to describe the generators
- Results from the lab experiments and computer simulations are presented, and compared.

1.3 Fault Ride Through Capability Requirements

The fault-ride-through assessment is based on a voltage against time-profile given in the network codes. The power generating modules have to be able to continue to produce stably after a grid fault as long as the voltage magnitude keeps above the given curve. National requirements have earlier been given for larger generation units, but will now also be given for DG units with rated capacities above 1.5 MW.

1.4 SINTEF DipLab

The fault ride through capability in small power plants are often unknown which in some areas makes it difficult to analyse the grid reliability [3]. SINTEF Energy Research has therefore with financial support from the Norwegian Research Council and different grid companies and producers started a project where a mobile high voltage lab has been purchased from FGH GmbH. The lab is used to perform short circuit tests on power plants up 10 MW to increase the knowledge and information about capabilities of Norwegian small scale hydro, and to increase the credibility of results from dynamic simulation models.

The lab consists of two containers, one with reactances and one with circuit breakers and switches. The reactances can be varied to decide the depth of the voltage dip, while the length is controlled by the switching system.

1.5 Simulation Tool and Model Limitations

For the data simulations, the power system simulation tool SIMPOW version 11.0 was used. SIMPOW is mainly used for dynamic simulations in the time domain, and analysis in the frequency domain. The simulations in this report were made in TRANSTA mode, which is a transient stability mode. For an increased power transmission capability and

an improved transient stability, TRANSTA is using phasor models to check and tune the regulators[4].

The OPTPOW-files were used to create a system with an optimal power flow solution, while the DYNPOW-file were used for the dynamic analyses.

The generator has a production equal to the nominal power for all cases where nothing else is specified. This may not be a realistic approach. The turbines were modelled as a constant mechanical power, and no turbine regulators were implemented in the simulations, as this is not common in small scale hydro.

Some of the work carried out by Tina Bystøl in her master thesis written in 2007 have been used. The Snåsa grid model used for simulations are based on this work, and models of the voltage regulators were also made in her thesis. There have been some problems with the cosϕ and VAr regulator modes. For most of the work in this thesis, the voltage regulator without a reactive power loop have been used.

1.6 Report Structure

The report begins with a short literature study.

Chapter 2: The FRT capability restrictions to be applied on small generation units operating at lower voltage levels are presented.

Chapter 3: Transient rotor angle stability and generation unit control systems are introduced.

Chapter 4: A short study of faults, with focus on the transient grid faults occurring in the Norwegian power grid are given. Some statistics are presented, and representative voltage dips measured in the Norwegian power system are shown. The statistics are mainly based on a spreadsheet where all faults reported to Statnett in the 1-22 kV grid in 2009-2013 are collected. The complete spreadsheet is excepted from public disclosure.

Chapter 5: The Snåsa grid model is presented, and the functions of the DipLab is described along with the simulation model implementation. The parameters used to describe the power plant Bruvollelva is given.

Chapter 6: The laboratory experiment setup and simulation model of the in-house lab is presented.

Chapter 7: Results from the Snåsa grid computer simulations are presented in chapter 7. That includes simulations of three phase symmetrical faults, with focus on the voltage angle alternations, and experimental results and simulations of the DipLab experiment.

Chapter 8: The results from the in-house lab is given, and compared to simulation results.

The results are followed by a discussion, conclusion, further work and appendices.

2 | Fault Ride Through Requirements

2.1 Motivation

As there traditionally have been only a few small power plants connected to the grid, they have been ignored regarding restrictions to keep the grid stable. As the amount of small production units increase, there might be periods where small plants provide enough energy to cover the demand. The larger plants with larger inertias and better qualifications to provide a stable grid will not be spinning, and therefore not be able to keep the power system in an optimal operational state. A generator disconnection may lead to a further decrease in voltage and frequency in the area, and cascading failures may happen. The need for new rules concerning power system stability has therefore increased, to make sure that the smaller plants will be designed to provide the necessary services.

The European Network of Transmission System Operators (ENTSO-E) is an organisation that represents 41 TSOs from 34 different countries across Europe. A working group consisting of members from ENTSO-E have for several years worked on some new technical requirements, to make sure that we in the future will be able to provide a secure power grid. For the generating units, a set of grid codes called Network Code on Requirements for Generators (NC RfG) have been framed, for all new generation units [5]. The regulations aim to optimize the overall efficiency and the total cost of the power system. The TSOs and DSOs are welcome to take regional differences into account when defining the grid codes. The requirements from ENTSO-E was published the 17th of May 2016, and a reference group consisting of Norwegian grid companies and power production companies will help Statnett to propose some national specifications that will be sent to NVE within the exit of 2016. The final grid codes will be implemented by the fourth quarter of 2019[6].

One of the requirements listed in the network codes concern the fault ride through capability, which describes the ability to continue to produce power after a voltage dip. A voltage dip is defined as a temporary voltage reduction below 90% of nominal voltage[7]. Already existing plants do not have to meet with the restrictions, unless National Regulatory Authority and the TSO decides otherwise. The network codes [5] states the following:

> *This Regulation should provide for ranges of parameters for national choices for fault-ride-through capability to maintain a proportionate approach reflecting varying system needs such as the level of renewable energy sources ('RES') and existing network protection schemes, both transmission and distribution.*

2.2 Implementation

The new ENTSO-E network codes divides the restrictions into multiple groups based on the rated power of the generator and the voltage level at the connection point. The goal is to minimize the possibility of a critical event, and since the significance of a fault will increase with the size of the generating unit, the restrictions will also be more extensive. The different classifications is described in table 2.1.

Table 2.1: *Generator classifications for the Nordic countries*
Source: *[5]*

Type	Voltage level	Capacity limit
A	$<$ 110 kV	$>$ 800 W
B	$<$ 110 kV	$>$ 1.5 MW
C	$<$ 110 kV	$>$ 10 MW
D	$>=$ 110 kV	$>$ 30 MW

The fault ride through capability requirements apply to the generating units classified as a type B or larger. Bruvollelva power plant, which is studied in this report is rated at 22 kV and 3.9 MW. It will therefore be classified as a type B.

The voltage profile is based on the phase-to-phase voltages at the connection point of the generating unit during a symmetrical fault. The network codes defined by ENTSO-E gives the national authorities and the TSOs the authority to define the voltage against time-profile for the specific country. The profile shall include both pre-fault and post-fault conditions. A lower and higher limit are written in the network codes. The TSO is in other words free to choose the requirements to let them fit the national standards, but the shape of the FRT curve is given as a template, seen in figure 2.1. The accompanying values for which the TSOs may choose within are shown in table 2.2. Fault-ride-through capabilities in case of asymmetrical faults shall be defined by each TSO.

Each power generating module have to be able to stay connected to the network, and continue to produce stably as long as the voltage is above the given line. U_{ret} is the retained voltage during the fault, while the three parameters called U_{rec} are the recovery voltages after the fault.

As seen in table 2.2, the TSOs are provided a spectre of parameters to choose from when deciding the FRT-curve. The upper and lower boundary is shown in the blue lines in figure 2.2. Today, only a few DG units have requirements concerning the FRT capability, but generation units connected to the regional and central grid with voltage levels above 132 kV have functional requirements stated in FIKS[8]. In figure 2.2, the restrictions for the Norwegian 132 kV grid is added as a orange line. A generator trip has more severe consequences in the higher voltage levels and for larger machines. The new restrictions relating to DG units will therefore most likely be less stringent than the line plotted in orange.

Table 2.2: *Parameters for figure 2.1*

Parameter	Value
U_{ret}	0,05-0,3
U_{clear}	0,7-0,9
U_{rec1}	U_{clear}
U_{rec2}	0,85-0,9 and $\geqslant U_{clear}$
t_{clear}	0,14-0,25
t_{rec1}	t_{clear}
t_{rec2}	t_{rec1}-0,7
t_{rec3}	t_{rec2}-1,5

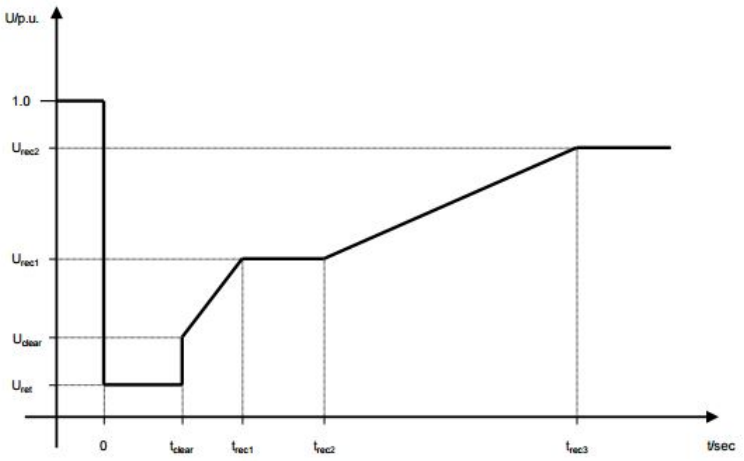

Figure 2.1: *FRT capability curve for Synchronous Power Generating Modules*
Source: *[5]*

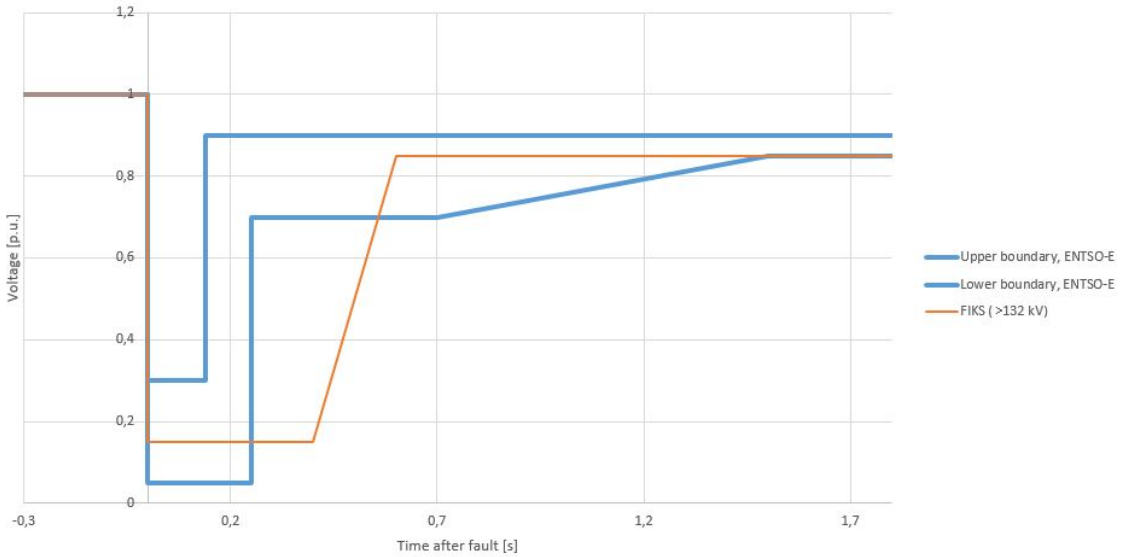

Figure 2.2: *Upper and lower boundaries for FRT capability curve for Synchronous Power Generating Modules in blue, FIKS requirements for units above 132 kV in orange*

The robustness of the network is highly dependent on the short circuit capacity. In addition to present a voltage-against time profile, the TSOs shall specify some pre-fault and post-fault conditions regarding minimum short circuit capacity, active and reactive power. The restrictions will not apply to generating units operating below these conditions[5].

3 | Power System Stability and Control

3.1 Power System Stability

Power quality is defined as the ability to meet with the demands concerning frequency, voltage and the level of reliability [9]. Power system stability refers to the property of a power system to keep an operating equilibrium under normal conditions, and to regain an acceptable state of operation after a physical disturbance. Since power system stability is a highly complex topic, Kundur[10] and others have chosen to divide the problem into three main groups. This is to easier be able to make proper simplifications when analysing stability issues. The three groups are divided based on the physical nature of the instability, the size of the disturbance and the time it takes to regain stability. The different groups and sub-groups are shown in figure 3.1. In this chapter, the phenomena rotor stability will be studied. The other types of stability mentioned in figure 3.1 are described in the project thesis report[2].

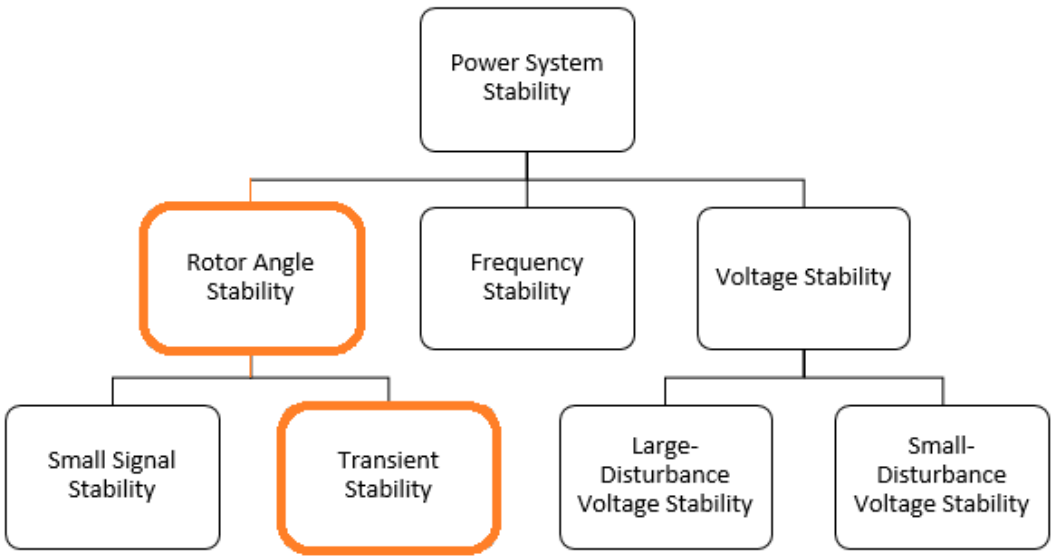

Figure 3.1: *Power System Stability Classifications*
Source: *Drawn with basis in the classifications from [9] and [10]*

3.2 Rotor Angle Stability

Maintaining a synchronous operation has always been important to avoid instability in the power system[9]. It is therefore necessary for the synchronous machines to stay in synchronism for the power system to stay stable. It is the dynamic relation between the generator rotor angle and power angle that influence this stability aspect. The ability of interconnected synchronous machines to stay within synchronism is called "Rotor Angle Stability".

As seen in figure 3.1, rotor angle stability can be divided into two sub-groups. The first is small-signal stability, which is caused by small variations in load or generation. The instabilities are so small that the system equations might be linearised, and yet permissible for analyses. Small-signal disturbances happens continually in the power system, creating an increase in rotor angle due to lack of torque synchronization, or oscillations in rotor angle with an increasing amplitude due to lack of damping torque[9].

When more severe transient disturbances occur in the power grid, the disturbance is classified under the sub-category transient stability. Both small signal stability and transient stability are categorized as short-term stability, meaning that the disturbances lasts for 0-10 seconds. The transient rotor angle stability is referring to more severe faults, often cleared by the opening of a circuit breaker or by isolation of a faulted component.

The post-disturbance operation point will often differ from the system pre-disturbance during a transient instability. The severity of the disturbance may vary, but the system should be designed to cope with contingencies such as different types of short circuits on transmission lines. The clearing time of the fault is an important factor when studying the transient rotor angle stability. This is described further in section 3.2.1.

Transient disturbances leads to large fluctuations in generator rotor angle. Equation (3.1) shows the power transferred from the generator as a function of generator and system voltage for steady state systems. All resistance are here neglected.

$$P = \frac{E_G V_S}{x_d} sin\delta + \frac{V_S^2}{2} \frac{(x_d - x_q)}{x_d x_q} sin(2\delta) \tag{3.1}$$

x_d is the total direct axis reactance, seen from the generator, and x_q the total quadrature axis reactance. This includes the generator reactance, generator transformer reactance and the system reactance. The equation is shown in (3.2) and (3.3). δ refers to the rotor angle, which is the difference between the voltage angle of the induced generator voltage (E_G) and the system voltage (V_S).

$$x_d = X_d + X_t + X_s \tag{3.2}$$
$$x_q = X_q + X_t + X_S \tag{3.3}$$

The second part of equation (3.1) is often neglected for round generators (where x_d=x_q) or when the system reactance is large, giving a large denominator. The difference between a "stiff" and a "weak" grid is the system reactance X_S. A weaker grid has a larger system reactance, leading to a larger total system reactance x_d. A generator operating in a weak grid will therefore have a larger component sinδ in steady state operation, as the produced power is the same as in a stiff grid. The steady state rotor angle will therefore be larger in a weaker grid.

The generator model change during a disturbance, as the reactances are different for a dynamic and a steady state system. The transient reactances can be written as in equation (3.4) and (3.5)

$$x'_d = X'_d + X_t + X_s \tag{3.4}$$
$$x'_q = X'_q + X_t + X_s \tag{3.5}$$

As the transient reactances are relatively small compared to the transformer reactance and the system reactance, the assumption $x_q \approx x_d$ can be made. Equation (3.1) can be rewritten and the generated power will follow equation (3.6). This equation is called the "Classical model".

$$P = \frac{E'_G V_S}{x'_d} sin\delta' \tag{3.6}$$

The power-delta function for steady state and transient case is shown in figure 3.2. α is the difference between δ and δ', which is zero for salient pole machines.

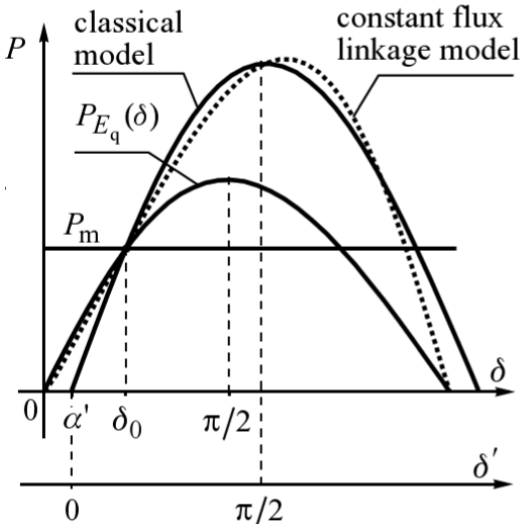

Figure 3.2: *Steady state and transient power-delta characteristics for laminated salient-pole generators*
Source: *[11]*

The power drawn from the generator may be written $P_{max}sin\delta'$ as the maximum transmitted power is when the sine equals one. The swing equation for transient stability can

be written:

$$\frac{2HS_n}{\omega_s}\frac{d^2\delta}{dt^2} = P_m - P_{max}sin\delta \tag{3.7}$$

Where P_m is the mechanical power delivered from the turbine.

3.2.1 Rotor Angle Behaviour During a Three Phase Fault

The method *Equal area criterion* can be used to analyse the consequences of a three phase fault [11]. Damping is neglected, and the change in speed is assumed to be so small that the turbine governor system will not be affected. A three phase fault causes a short circuit on the specific bus, and the voltage becomes zero. The voltage will stay zero until the fault is cleared. The progress is sketched in point 1-2-3 in figure 3.3, which shows the power as a function of the power-angle and the variation of power angle in time for a short and a long fault clearing time. When the fault is cleared, the voltage will rise to the characteristic given in the figure, and kinetic energy proportional to the area between 1-2-3-4 will occur in the rotor. The rotor torque will start decelerating back to the state it had before the fault, but because of the kinetic energy, the angle will continue to increase until all developed energy has been used. This corresponds to the area 4-5-6-7, which in part (a) of the figure has the same area as 1-2-3-4. The cycle will repeat until a steady state is reached, and the rotor will swing back and forth performing synchronous swings, which eventually will be damped.

For the system (b) to the right, the clearing time is longer. As seen in the figure, the mechanical power P_m is reached before all the kinetic energy gained during the fault is absorbed. As a result, there will be a speed deviation, and the power angle will continue to increase. The rotor will experience an asynchronous rotation, and the synchronism is lost.

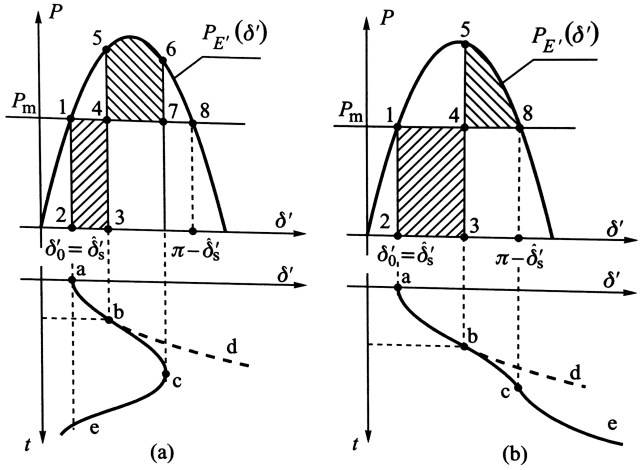

Figure 3.3: *Power as a function of power-angle with acceleration and deceleration area shaded and power-angle as a function of time for (a) a short and (b) long clearing time*
Source: *[11]*

3.3 Generating Unit Control

To maintain a stable power system, power system controls are implemented, and the power flow is scheduled to endure contingencies. This section describes the basic behaviour of the control systems of the generating unit. Other power system control systems are described in the specialization project report [2].

Both frequency and voltage have to be within given boundaries for the power system to be in a stable operating state. Both voltage and speed controls are therefore connected to the production units to keep the system within required boundaries as the operational state in the surrounding grid has changed. A block diagram of a power plant with excitation system is given in figure 3.4, where the generator is showed together with an automatic voltage regulator, exciter and turbine governor.

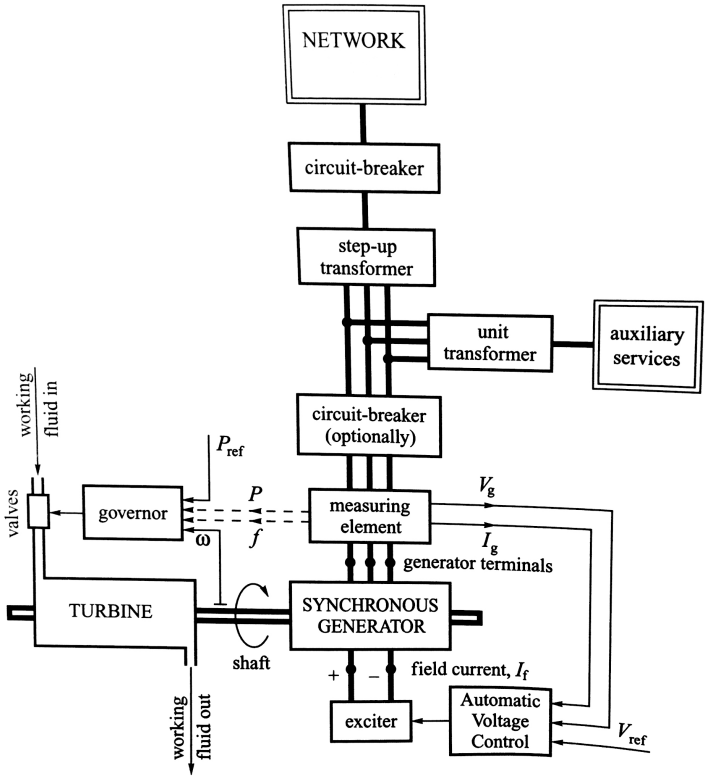

Figure 3.4: *Block diagram of a power plant with control system*
Source: *[11]*

3.3.1 Exciter

The main purpose of an exciter is to provide a DC current in the field windings, creating a rotating flux and a field voltage. The field voltage creates a current in the armature windings, and consequently a terminal voltage. How much current that is flowing in the field windings is decided by the automatic voltage regulator (AVR). The exciter receives a signal from the AVR, and the current is adjusted up or down. There are two main

excitation systems. The DC source may be external, supplying the field windings with a DC current utilizing slip rings. The DC source may also be on the same rotating shaft as the generator rotor. An AC machine creates a current, which is rectified before it is supplied to the field windings.

A brushless AC excitation system is showed is figure 3.5. A permanent magnet pilot exciter creates an AC current, which is rectified before reaching the exciter.

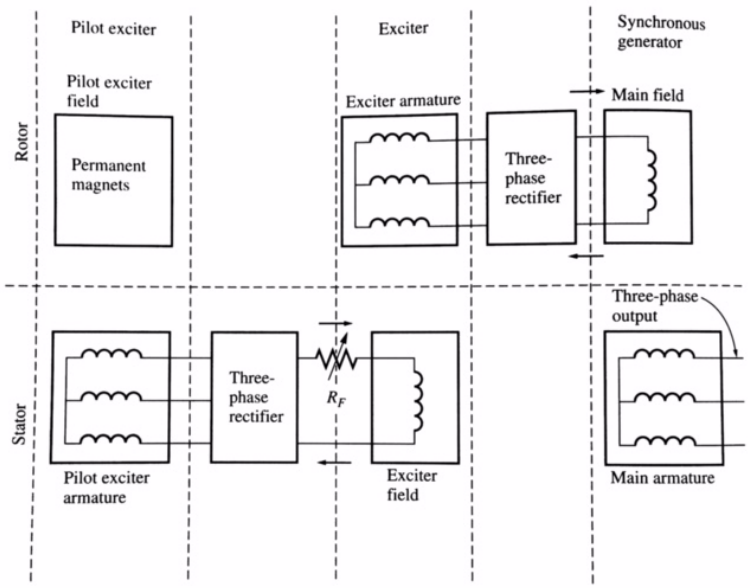

Figure 3.5: *A brushless excitation system with a pilot exciter*
Source: *[12]*

3.3.2 AVR

An AVR has a measuring element placed on the generator terminals. The current flowing from the generator, terminal voltage and frequency is measured. The measured voltage level is registered, and compared to a reference voltage in the AVR. The voltage error is then amplified, and the signal is sent to the exciter.

A block diagram of a Basler DECS 200 is shown in figure 3.6. This is a digital PID regulator, with both integrator and derivation effect. The AVR is compact, yet effective, and is therefore commonly used on synchronous generators in DG units.

Some regulators do have an additional VAr or cosϕ control. The AVR is then supplied with an additional signal, as the active and reactive power is measured on the generator terminals. The signal is compared with a reference in the AVR, and the excitation current is regulated the same way as the voltage deviations. The controller is implemented as a slow PI regulator, making the outer loop of a two loop system[13]. The VAr- and cosϕ controller for the Basler DECS-200 is shown in in figure 3.7 and 3.8

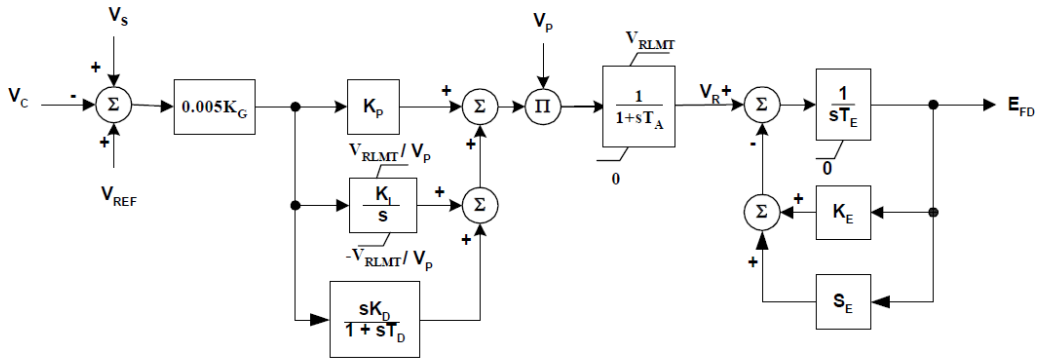

Figure 3.6: *Block diagram of a Basler DECS 200*
Source: *[13]*

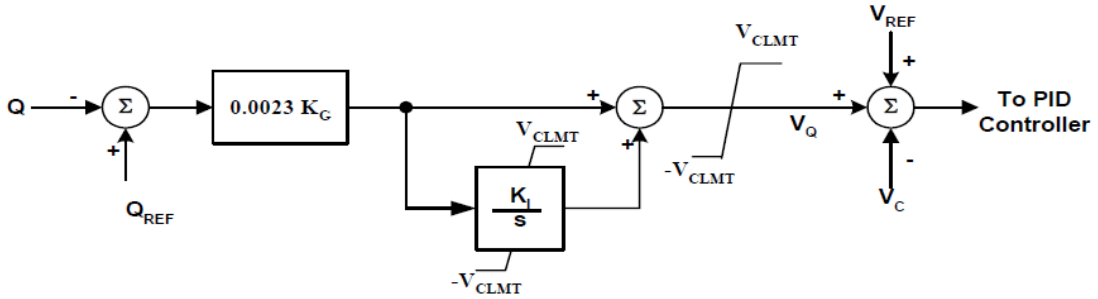

Figure 3.7: *Block diagram of a VAr controller in Basler DECS 200*
Source: *[13]*

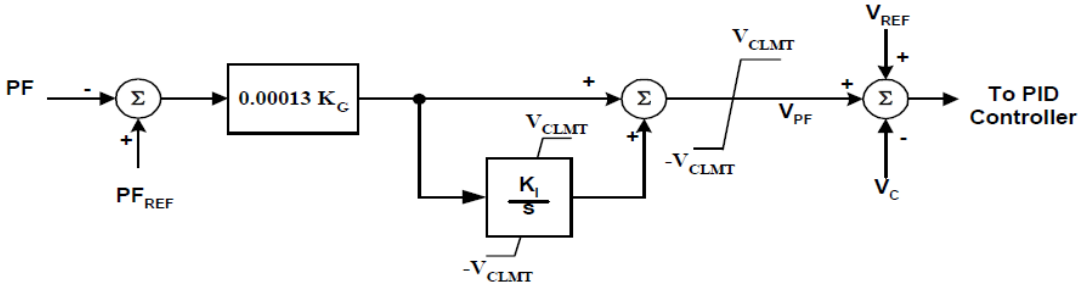

Figure 3.8: *Block diagram of a cosϕ controller in Basler DECS 200*
Source: *[13]*

3.3.3 Power System Stabilizer

The power system stabilizer (PSS) is used to provide additional control to the AVR and the Governor. PSS is used to damp the low-frequency oscillations appearing after a disturbance. Signals from machine speed, terminal frequency or power are processed through the PSS, with a transfer function G(s) [14]. The transfer function includes a positive feedback, and places the poles such that the damping is reduced. The output signal is added to the AVR signal and sent to the exciter, to control the field voltage.

This kind of control is not implemented in the simulation models in this report, as it is not a part of the control system at the DG unit studied.

3.3.4 Turbine Governor

The speed of the prime mover is decided by the frequency in the grid and the number of poles in the generator. When studying the power system dynamics, approximate linear models are used to capture the impact of the plant on the electrical system[14]. The turbine torque and the speed control are of interest, as they directly influence the power system. Automatic speed control is therefore used to control the frequency and voltage on the generator terminals. A valve control is provided by a speed sensor, a hydraulic amplifier and a piston. Turbine governors have for many years been of mechanical-hydraulic type, but today electro-hydraulic governors are mostly used[11]. The main difference between the two types is that the rotor speed is measured electronically, giving a higher accuracy. Turbine governors are not common for distributed generation units.

4 | Faults

Any failure that interferes with the normal flow of current is defined as a fault. There are many causes of a failure, but the result is often a flashover between a various number of conductors and a grounded part of the system, creating a short circuit. The fault might also be between two or all three of the conductors without connection to ground.

4.1 Symmetrical Components and Sequence Networks

The method of symmetrical components was introdued by C.L. Fortescue, and is based on the fact that an unbalanced system with n phasors always can be resolved into n balanced systems. [15] A three phase system with three unbalanced phasors, can be resolved into a positive-, negative and zero- sequence component. The positive and negative sequence consists of three phasors with equal length and 120° shift in phase. The Zero sequence components are also equal in magnitude, but has zero phase displacement from each other. The unbalanced system of phasors will be the sum of each of the three sequences, as seen in figure 4.1 and 4.2.

$$V_a = V_a^{(0)} + V_a^{(1)} + V_a^{(2)} \tag{4.1}$$
$$V_b = V_b^{(0)} + V_b^{(1)} + V_b^{(2)} \tag{4.2}$$
$$V_c = V_c^{(0)} + V_c^{(1)} + V_c^{(2)} \tag{4.3}$$

Since the positive and negative sequence components are displaced with 120° from each other, while the zero sequence phasors are in phase, the equation (4.1)-(4.3) can be written

$$\begin{bmatrix} V_a \\ V_b \\ V_c \end{bmatrix} = \begin{bmatrix} 1 & 1 & 1 \\ 1 & a^2 & a \\ 1 & a & a^2 \end{bmatrix} \begin{bmatrix} V_a^{(0)} \\ V_a^{(1)} \\ V_a^{(2)} \end{bmatrix} = A \begin{bmatrix} V_a^{(0)} \\ V_a^{(1)} \\ V_a^{(2)} \end{bmatrix} \tag{4.4}$$

where a equals a phase shift of 120°.

Figure 4.3 show the different voltage phasors for each sequence, and also the total voltage in the point of fault for various types of faults. As seen in the first row, a three phase fault will result in a voltage equal to zero, and creating a "worst case" voltage dip.

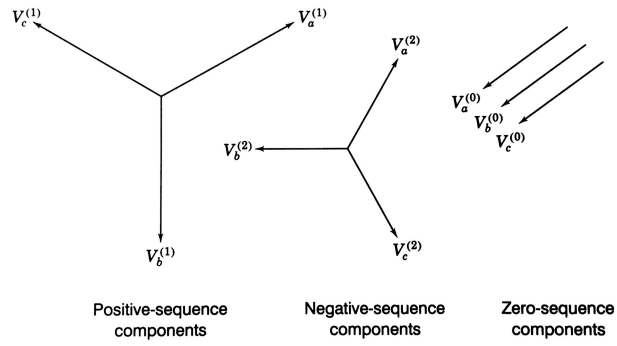

Figure 4.1: *Three sets of balanced phasors, divided into positive, negative and zero sequence components*
Source: *[15]*

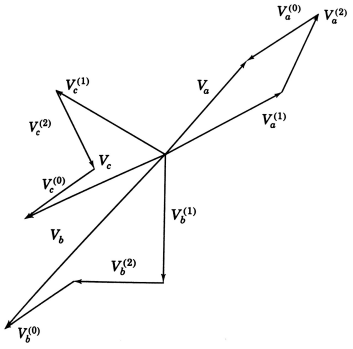

Figure 4.2: *Positive, negative and zero sequence components added to obtain three unbalanced phasors*
Source: *[15]*

Fault type	Positive sequence	Negative sequence	Zero sequence	Fault voltages
a,b,c	V_{a1}, V_{c1}, V_{b1}			Zero at fault
a,b	V_{a1}, V_{c1}, V_{b1}	V_{b2}, V_{c2}, V_{a2}		$V_a = V_b$, $V_c = V_a$
b,c	V_{a1}, V_{c1}, V_{b1}	V_{a2}, V_{b2}, V_{c2}		$V_b = V_c$
c,a	V_{a1}, V_{c1}, V_{b1}	V_{c2}, V_{a2}, V_{b2}		$V_a = V_c$, V_b
a,b,G	V_{a1}, V_{c1}, V_{b1}	V_{b2}, V_{c2}, V_{a2}	$V_{a0} = V_{b0} = V_{c0}$	$V_a = V_b = 0$, V_c
b,c,G	V_{a1}, V_{c1}, V_{b1}	V_{a2}, V_{b2}, V_{c2}	$V_{a0} = V_{b0} = V_{c0}$	V_a, $V_b = V_c = 0$
c,a,G	V_{a1}, V_{c1}, V_{b1}	V_{C2}, V_{a2}, V_{b2}	$V_{a0} = V_{b0} = V_{c0}$	$V_a = V_c = 0$, V_b
a,G	V_{a1}, V_{c1}, V_{b1}	V_{c2}, V_{b2}, V_{a2}	$V_{a0} = V_{b0} = V_{c0}$	$V_a = 0$, V_b, V_c
b,G	V_{a1}, V_{c1}, V_{b1}	V_{b2}, V_{a2}, V_{c2}	$V_{a0} = V_{b0} = V_{c0}$	V_a, V_c, $V_b = 0$
c,G	V_{a1}, V_{c1}, V_{b1}	V_{a2}, V_{c2}, V_{b2}	$V_{a0} = V_{b0} = V_{c0}$	V_a, $V_c = 0$, V_b

Figure 4.3: *Voltage phasors for each sequence and the total voltage at the point of fault for different types of faults. Z1=Z2=Z0, and magnitudes are not to scale.*
Source: *[16]*

4.2 Transient Grid Faults in the Norwegian Power Grid

Faults in the power grid may be caused by a variety of reasons. Induced voltages from lightning or direct lightning strikes are common reasons for short circuit faults. Another cause of faults is falling trees often provoked by wind, snow or other weather conditions. This is especially a problem in the distribution grids, as the lines usually cross areas with a higher density of trees. As heavy loading may cause heating in the lines, creating expansion and sagging of lines, trees are most likely to fall on the lines during high load periods[16]. A fault during a heavy load period makes the fault even more severe.

According to the book "Protective Relaying - Principles and Applications"[16], about 3/4 of the faults in the power system are single phase to line faults, and only 2-3% are three phase faults. An overview of the different fault types and the share of total amount of fault is seen in table 4.1.

Type of fault	Share of total
Single phase-to-ground	70-80%
Phase-to-phase-to ground	10-17%
Phase-to-phase	8-10%
Three-phase	2-3%

Table 4.1: *Approximate percentages of fault occurrence*
Source: *[16]*

The statistics above gives an approximate picture of all the faults occurring in the power grid, regardless of voltage level and duration. The statistics are not from the Norwegian grid, so the numbers may differ from the faults caused by Norwegian weather conditions.

As mentioned, trees tend to fall more often in the distribution grid than in the higher voltage levels. In this project, only temporary faults creating voltage dips with a short duration are relevant. Statnett keeps statistics for all the faults reported in the Norwegian power grid. With the fault statistics from the 22 kV grid between 2009 to 2013 as a source[17], temporary faults were selected and divided into three different groups. The first group are earth faults, which happen when there is a connection between one of the voltage carrying lines and earth. The second group are short circuit faults, which are faults where minimum two of the lines are involved. These kinds of faults may or may not involve ground. The final type is discharges. This kind of fault is mostly a result of over voltages caused by lightning. The current is lead to earth through a diverter, which creates a situation similar to a short circuit fault with earth connection. The occurrence of each type of fault can be seen in table 4.2.

Comparing table 4.1 and 4.2, one can see that almost half of the transient faults registered in the 22 kV grid involved minimum 2 phases, while only 2-3% of the total amount of faults did. The fault duration is unfortunately not taken into account in neither of the tables. Helge Seljeseth is a senior analyst within fault analysis at Statnett SF. He elaborated that

Type		Number of faults	Share of total
Earth faults (1phg)		4509	50%
Short circuits (2-3 phases)			
	With ground connection	1733	19%
	Without ground connection	1502	17%
	Unspecified	1017	11%
Discharges		252	3%

Table 4.2: *Reported faults in the Norwegian 22 kV grid 2009-2013*
Source: *[17]*

voltage dips in the low voltage grid might be caused by faults in the higher voltage levels. Most of the faults in the distribution grid is though a result of a fault in the distribution grid it self. A lot of the voltage dips are caused by unplanned loads suddenly connected to the grid, but the voltage reductions in these cases are usually longer than the ones studied as transient instability. Some examples of typical voltage dips logged in the Norwegian distribution grid is showed in figure 4.4-4.7.

The faults that will be studied in this paper are short circuit faults happening in the low voltage grid. As about 50% of the faults in the Norwegian distribution grid involve more than one phase, three phase to ground faults will be used for the simulations as this is the "worst case", and will therefore give realistic, but conservative voltage dips.

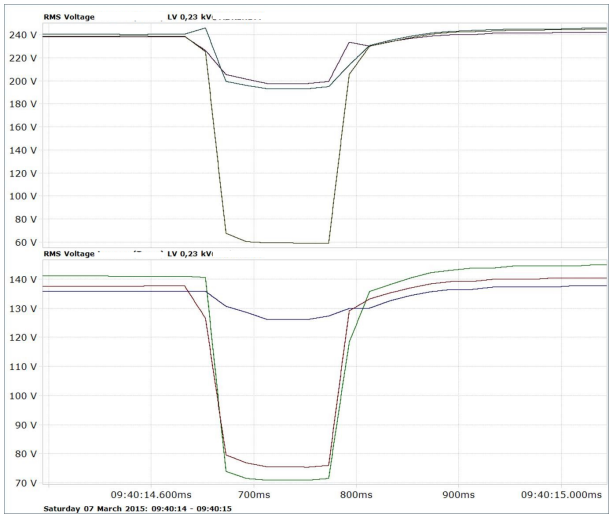

Figure 4.4: *Voltage dip with origin in the higher voltage levels*
Source: *[18]*

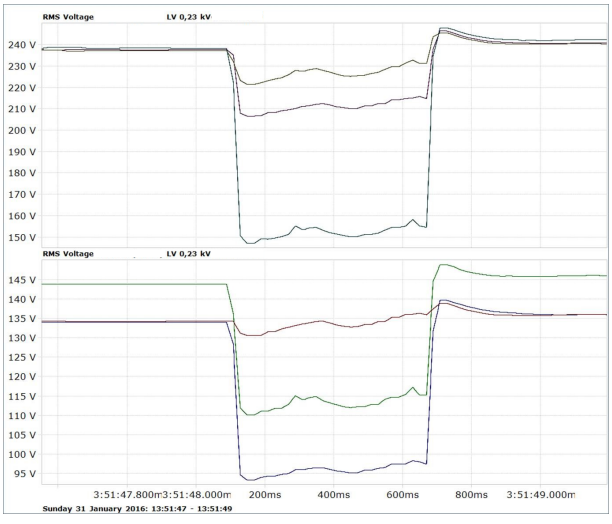

Figure 4.5: *Voltage dip with origin in the distribution grid*
Source: *[18]*

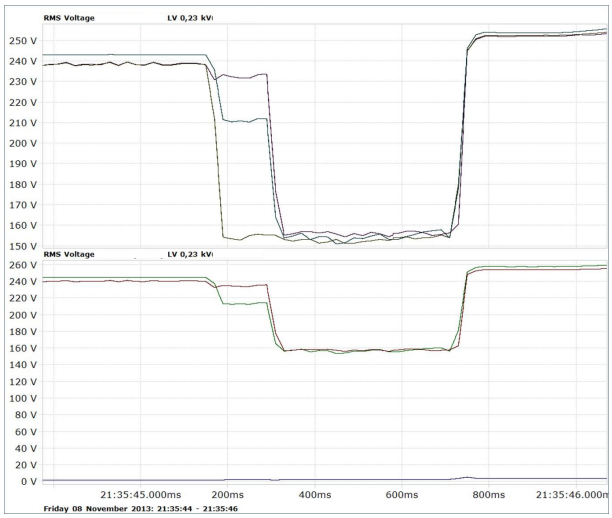

Figure 4.6: *Evolving voltage dip*
Source: *[18]*

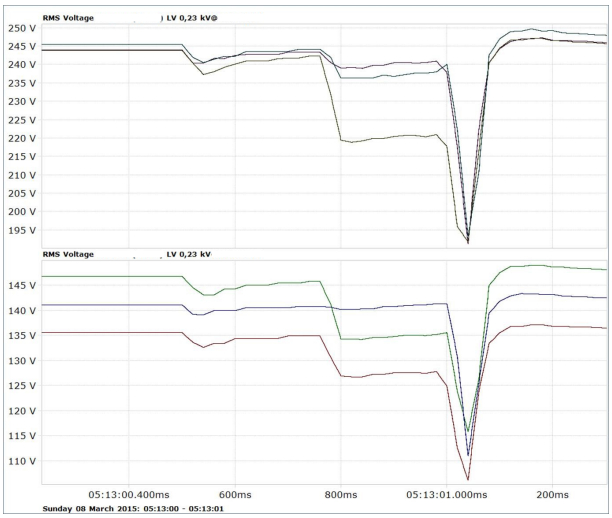

Figure 4.7: *Evolving voltage dip*
Source: *[18]*

4.3 Fault Impedance

When faults happen at or near a bus, the self admittance matrix change. Ground faults on lines will usually result in a flashover. An arc appear, and the total current path impedance will include the arc resistance, tower impedance and the impedance between the tower foundation and earth (tower footing resistance)[16]. The arc resistance will vary during the fault, and starts with a typical value between 1 and 2 Ω excising for about 0.5 seconds. The impedance will then increase, and the peak will be about 25-50 Ω. The footing impedance will vary for different towers, and may be less than 1 Ω, or up to several hundreds ohms. A simulation model of the impedance is therefore difficult to choose. A common assumption is that the fault impedance is approximately all real. Since the faults simulated in this project is mostly shorter than 0.5 seconds, the arc resistance is assumed to be so small that it can be neglected.

5 | Snåsa Test Grid - Model Description

5.1 Grid Model

Under studies of realistic faults, a model of the Snåsa grid was used. The grid model was made by Tina Bystøl in her master thesis "Stabilitetsporblemer i distribusjonsnett med lokal kraftproduksjon"[19] from 2007. The thesis studied stability issues caused by local power production in the distribution grid, and a model of the Snåsa grid was made in SIMPOW. Bruvollelva Power Plant, which is studied in this paper, was one of five DG units planned in this area at the time the model was made. Bruvollelva is referred to as DG1 in the model. Gravbrøtfoss power plant was built in 2019, and is a 2.1 MW hydro power plant with a synchronous generator, based on run of river[20]. This matches the description of DG4 in the model. According to wikipedia[21], there are no other DG units in the area. DG2, DG3 and DG5 are therefore excluded from the original model in this project.

The grid model included a swing bus at 66 kV, connected to a 22 kV grid through a transformer. DG4 was operating at 690 V, and DG1 at 6.6kV. DG1 was placed closer to the swing bus than DG4. As seen in appendix A.1, the short circuit capacity measured at the connection point of DG1 is 125 MVA[22]. This was modelled as an internal impedance on the swing bus with a ratio 1:10 between the reactive and active part. There were also multiple loads connected to the grid. All the loads were in the optimal power flow modelled with a voltage exponent for active power equal to 1, making a change in power demand proportional to the voltage change. This is seen in equation (5.1). In the dynamic model, the power exponents were 2 by default. The loads in the dynamic simulations were therefore modelled as resistive loads, making the relative change in power demand squared proportional to the change in voltage.

$$P_{load} = P_{load,0}(\frac{U}{U_0})^{MP} \tag{5.1}$$

A single line diagram of the grid model with optimal power flow is shown in figure 5.1, and the optpow and dynpow files used in SIMPOW are attached in appendix D.1.

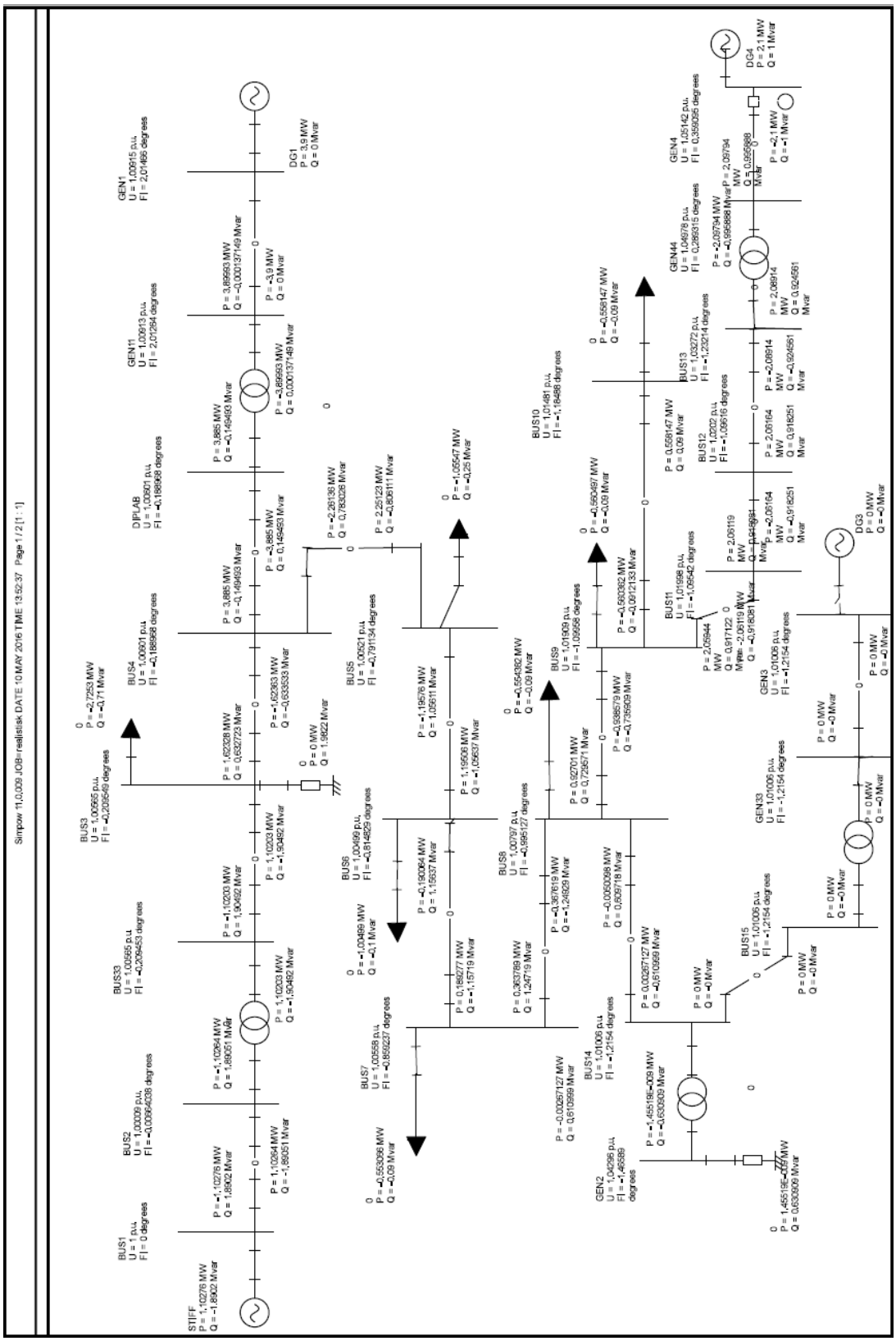

Figure 5.1: *Single line diagram of the Snåsa grid model*
Source: *[19]*

5.2 Method for Testing the Voltage Angle Influence on Fault Ride Through Capability

When a three phase fault occur somewhere in the system, the voltage at the generator terminals will be affected. The voltage amplitude change, and so does the voltage angle. However, the requirements for fault ride through are only related to the voltage magnitude. In section 7.1.2, the impact of the voltage angle in the fault ride through capability assessment is studied. Three phase faults are implemented on different nodes, and the critical clearing time of the power plant is studied. The voltage magnitude during the realistic fault is saved, and then implemented on the generator terminals. The voltage seen by the generator will be the same as during a realistic fault, but the voltage angle will not be affected to the same extent. The duration of the fault will then be adjusted manually to find the critical clearing time without the voltage angle contribution. The dynpow file is seen in appendix D.2

5.3 DipLab

The DipLab is a mobile short circuit lab consisting of two containers, operating at a voltage level below 33 kV. A picture of the lab is shown in figure 5.2. The container to the left consists of SF_6 and vacuum switches, epoxy isolated voltage transformers, current transformers and overcurrent diverters. This is where the length of the dip is controlled. The container to the right consists of 24 reactances, where 12 are meant to create a series reactance, and 12 are ment to create a short circuit reactance in parallel with the generating unit. There are also over current diverters connected to the reactors [23].

Figure 5.2: *Picture of the SINTEF DipLab outside Bruvollelva power plant at Snåsa*

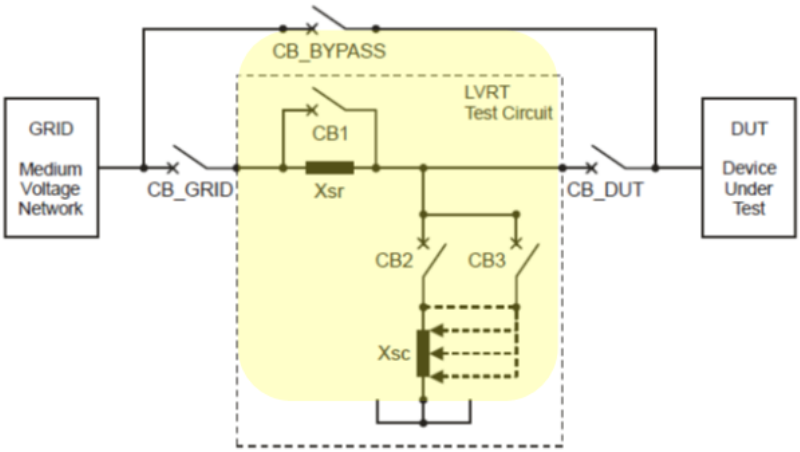

Figure 5.3: *Simplified one line diagram of the dip lab*
Source: *[23]*

A diagram of the lab is shown in figure 5.3, where X_{sr} is the series reactor and X_{sc} is the short circuit reactor. The 24 reactors are coupled such that each phase get four reactors creating the series reactance, and four creating the shunt. The series reactances are coupled per phase, and the short circuit reactances are star connected. The reactances can be adjusted by changing how many inductances that are in use per phase.

The circuit breaker referred to as CB_{Bypass} in figure 5.3 is meant to keep the plant connected to the grid when the test is not running. When the test is implemented, CB1 is connected, and CB_{GRID} and CB_{DUT} is then connected at the same time as CB_{BYPASS} is disconnected. This means that the power is flowing from the test object to the grid through CB1. CB1 is then disconnected so that the current is flowing through the series reactance. The short circuit reactance is connected by closing CB2 and/or CB3. Most of the current will pass through the shunt causing a voltage drop. When the test-period is over, CB2 and CB3 are disconnected and CB1 is connected. Because of the series reactance, the grid will not experience the same voltage drop as the power plant.

Further information about the lab and the laboratory equipment can be found in the report written by SINTEF Energy research "Testing av småkraftverks FRT-egenskaper"[1].

5.3.1 DipLab Simulation Model Description

The DipLab was modelled in the Snåsa grid model to make simulations comparable to the measured results. In that way, the simulation model could be verified and improved for better computer based studies. The DipLab was modelled between two nodes in the Snåsa grid model. A single line diagram can be seen in figure 5.4, and the optpow and dynpow files are attached in appendix D.3. One inductor was placed in series with the generator transformer and the external grid, short circuited by the already existing line. An other inductor was placed in parallel with the generator. A switch was placed between the generator terminals and the shunt inductor. When running the lab, the line in parallel

with the series inductor was disconnected. Five seconds later, the switch connecting the shunt reactance was closed, creating a three phase short circuit. The switch was then opened to clear the fault. Finally, the line was reconnected one second later.

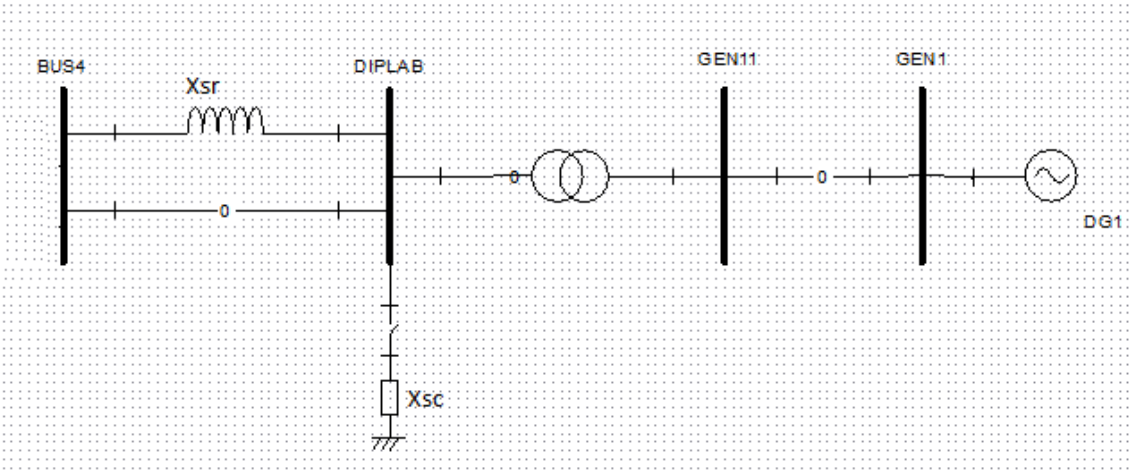

Figure 5.4: *Single line diagram of the SINTEF DIPLAB*
Source: *[23]*

5.4 Bruvollelva Power Plant

Bruvollelva power plant was used by SINTEF Energy Research when testing the DipLab in April 2016, which is placed in Snåsa in Nord-Trønderlag. The power plant has a salient pole synchronous generator produced by the Croatian company Koncar with rating 4335 kVA and 6.6 kV. The turbine is a horizontally installed francis turbine, with installed capacity of 3.9 MW.

Figure 5.5: *Bruvollelva Power Plant*
Source: *[24]*

5.4.1 Generator Parameters

The excitation system is brushless, and the nominal speed is 750 rpm. The generator parameters were found during the work with the project thesis [2], and are based on a data sheet from the power company Småkraft. The data sheet is attached in appendix A.2. Table 5.1 shows the parameters used for the simulations.

Table 5.1: *Generator data for Bruvollelva*

Parameter	Description	Value
Name		6SBV6 710M1-8
S_N	Rated power	4.335 MW
$\cos\phi_N$		0.9
n	Speed	750 rpm
H	Inertia constant	0.370 s
J	Moment of inertia	520 kgm^2
X_d	Direct axis reactance	2.36 pu
X'_d	Direct axis transient reactance	0.249 pu
X''_d	Direct axis subtransient reactance	0.161 pu
X_q	Quadrature axis reactance	2.32 pu
X'_q	Quadrature axis transient reactance	2.32 pu
X''_q	Quadrature axis subtransient reactance	0.189 pu
T_A	Armature time constant	0.067 s
R_A	Armature resistance	0.0068 pu
X_A	Leakage reactance	0.151 pu
T'_{d0}	Direct axis transient open-circuit time constant	1.750 s
T''_{d0}	Direct axis subtransient open-circuit time constant	0.092 s
T''_{q0}	Quadrature axis subtransient open-circuit time constant	0.090 s
T'_d	Direct axis transient time constant	0.184 s
T''_d	Direct axis subtransient time constant	0.059 s
T''_q	Quadrature axis subtransient time constant	0.007 s
R_0	Zero sequence resistance	0.0069 pu
X_0	Zero sequence reactance	0.092 pu

The saturation parameters describes for which level of field voltage the machine reaches saturation. This is given in a saturation curve where the non-linear relation between current and voltage is described. The saturation curve is not given for this machine, and the values used in the project report are therefore used.

Table 5.2: *Saturation data for the Bruvollelva generator*
Source: *[19]*

Parameter	Value
V1D	1,0
V2D	1,2
SE1D	0,1
SE2D	0,3

5.4.2 Voltage Regulator Parameters

The voltage regulator at Bruvollelva is a Basler DECS 200 with possibilities of AVR, VAr-mode and power factor-mode. The block diagrams for the controller with options for cosϕ and VAr modes are shown in figure 3.6, 3.7 and 3.8 The parameters for gains and time constants for the voltage regulator were found by reading of the AVR on site. The settings are given in table 5.3. VAr-mode was used when the machine was starting up, while PF-mode (cosϕ) was used during normal operation. The values for voltage limitations and saturation curves are the same as Tina Bystøl used[19]. The parameters are given in table 5.4.

Table 5.3: *AVR Settings used at Bruvollelva*

Regulator type	Parameter	Value
AVR:	K_p	177.2
	K_i	148.5
	K_d	66.3
	T_d	0.08 s
VAR:	K_i	10.0
	K_g	1.0
	Var-mode	0.00 VAr
Cosϕ:	K_i	3.0
	K_g	1.0
	PF-mode	0.990 cap

Table 5.4: *Additional AVR parameters used in the simulation model*

Parameter	AVR	VAR	Cosϕ
VRmin	0	0	-1
VRmax	35	10	10
Ymin	-	-0.1	-0.1
Ymax	-	0.1	0.1
Vmin	-	-0.1	-0.1
Vmax	-	0.1	0.1
E1	2.222	2.222	2.222
SE1	1.346	1.346	1.346
E2	2.962	2.962	2.962
SE2	1.9	1.9	1.9
TE	0.5	0.5	0.5
KE	1.0	1.0	1.0
TA	0	0	0
KA	1.0	1.0	1.0

5.4.3 Protection

Distributed generators may experience hazards and problems such as internal faults (short circuits or ground faults in the stator or rotor), system disturbances and operational faults. This can include problems such as loss of prime mover, overexcitation, nonsynchronized connection to the grid, thermal overload and others[16]. Additional protection is therefore required at the point of common coupling for the distributed generator and the main grid. The AVR at Bruvollelva provides a list of protection units. The different protections and limiters are listed in table A.1 and A.2.

6 | In-House Lab - Model Description

6.1 Laboratory Experiment Setup

The in-house laboratory model was a 1 kW synchronous generator with a synchronous machine as a prime mover. The generator was connected to the local 400 V grid through an inductor. During the experiments, another inductor was connected and then disconnected to the generator terminals by help of a solid state relay, creating a short circuit reactance. The relay was initially open, then closed for a given amount of time, before it was reopened. A signal generator controlled the relay. For some of the experiments a long cable was placed between the grid and the series inductor to make the grid connection weaker. The lab machine and prime mover is pictured in figure 6.1, and the list of equipment is given in appendix C.

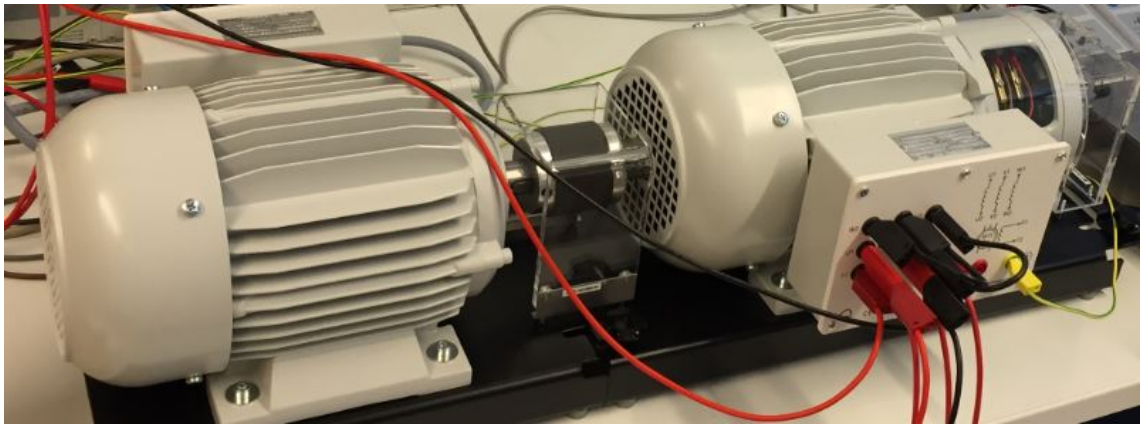

Figure 6.1: *Lab machine and prime mover*

The generator used was of type Leybold class 1.0 without any kind of voltage regulation. There was no information about the generator parameters in the manual, and the producer of the machine was contacted to get a data sheet for the machine without any response. Some measurements and tests were therefore made to get necessary parameters for the simulations. The lab machine was a salient pole machine with damper windings. The parameters used for the simulations are shown in table 6.1. The different parameters are calculated in chapter B in the appendix.

The cable used between the grid and the series inductor was a 3 phase PR cable with a

Table 6.1: *Synchronous generator parameters for the in-house lab machine*

Parameter	Description	Value
S_n	Rated power	1 kW
U_n	Rated voltage	400 V
H	Inertia Constant	0.094 s
D	Damping Constant	0
X_d	Direct axis reactance	0.78 p.u.
X'_d	Direct axis transient reactance	0.29 p.u.
X''_d	Direct axis subtransient reactance	0.10 p.u.
X_q	Quadrature axis reactance	0.507 p.u.
X'_q	Quadrature axis transient reactance	0.0.507 p.u.
X''_q	Quadrature axis subtransient reactance	0.10 p.u.
T'_{0d}	Direct axis transient open-circuit time constant	0.039 s
T''_{0d}	Direct axis subtransient open-circuit time constant	0.012 s
T'_{0q}	Quadrature axis transient open-circuit time constant	0.039 s
T''_{0q}	Quadrature axis subtransient open-circuit time constant	0.012 s
R_A	Stator Resistance	0.066 p.u.
X_A	Leakage reactance	0.08 p.u.

diameter of 1.36 mm, giving a cross-section area of $1.5mm^2$. The resistance was measured with a milliohm meter, and equalled 270 mΩ per phase. Since the cable consisted of copper only, a data sheet for copper was used to calculate the cable reactance. A three core cable of copper have a resistance of 15.1 Ω per km and reactance of 0.118 Ω per km[25]. The reactance per phase is calculated in (6.2)

$$R_{cable} = 270m\Omega \tag{6.1}$$

$$X_{cable} = \frac{0.118}{15.1} \cdot 270m\Omega = 2.11m\Omega \tag{6.2}$$

6.2 Simulation Model

The lab was modelled as a simple four bus system, seen in figure 6.2. The swing bus is placed on BUS1, with a voltage of 1 per unit and a voltage angle equal to zero. The lab machine is modelled on node BUS4. The optpow and dynpow files are attached in appendix D.4. The generator torque was adjusted by changing the active power from the generator, calculated by use of equation (6.3).

$$\tau = \frac{P}{\omega} = \frac{P}{2\pi\frac{n}{60}} = \frac{P}{50\pi} \tag{6.3}$$

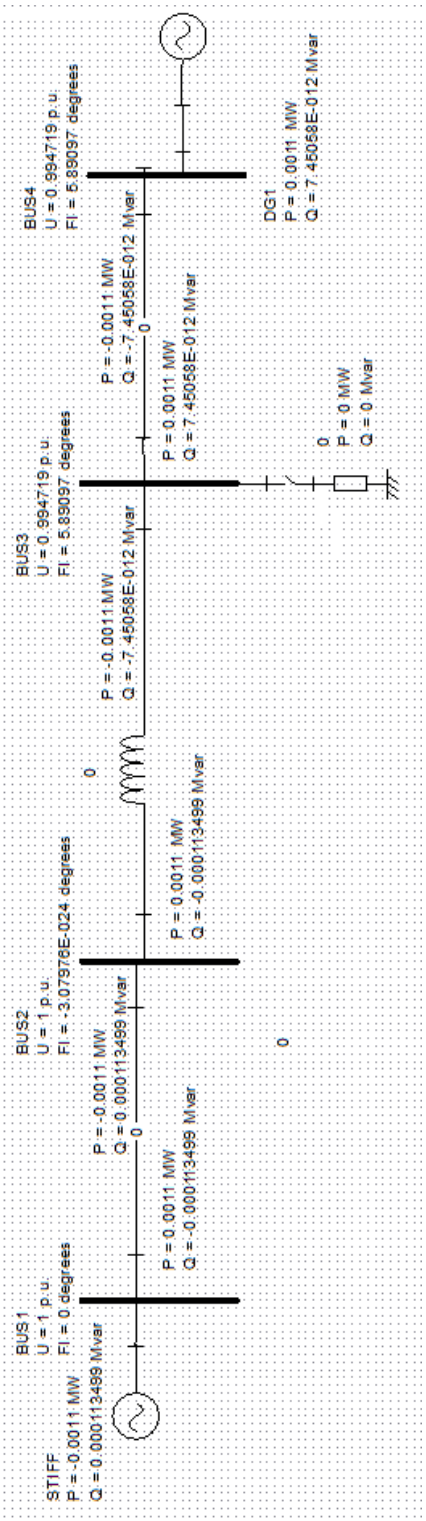

Figure 6.2: *Single line diagram of the in-house lab simulation model with optimal power flow at nominal power*

7 | Results - Field Experiments and Data Simulations from Snåsa

7.1 Realistic faults

7.1.1 Voltage Dips During Realistic Faults

To study realistic "worst case" faults, three phase faults were implemented in the Snåsa grid model, and a voltage dip was studied on multiple nodes. Figure 7.1 shows how a three phase to ground fault at node BUS7 will create dips in voltage magnitude in the surrounding grid. The power plant called DG1 (Bruvollelva) was simulated with a cosϕ regulator, as in the actual power system. DG4 was simulated with the simplest AC8B-regulator, without VAr or cosϕ-mode.

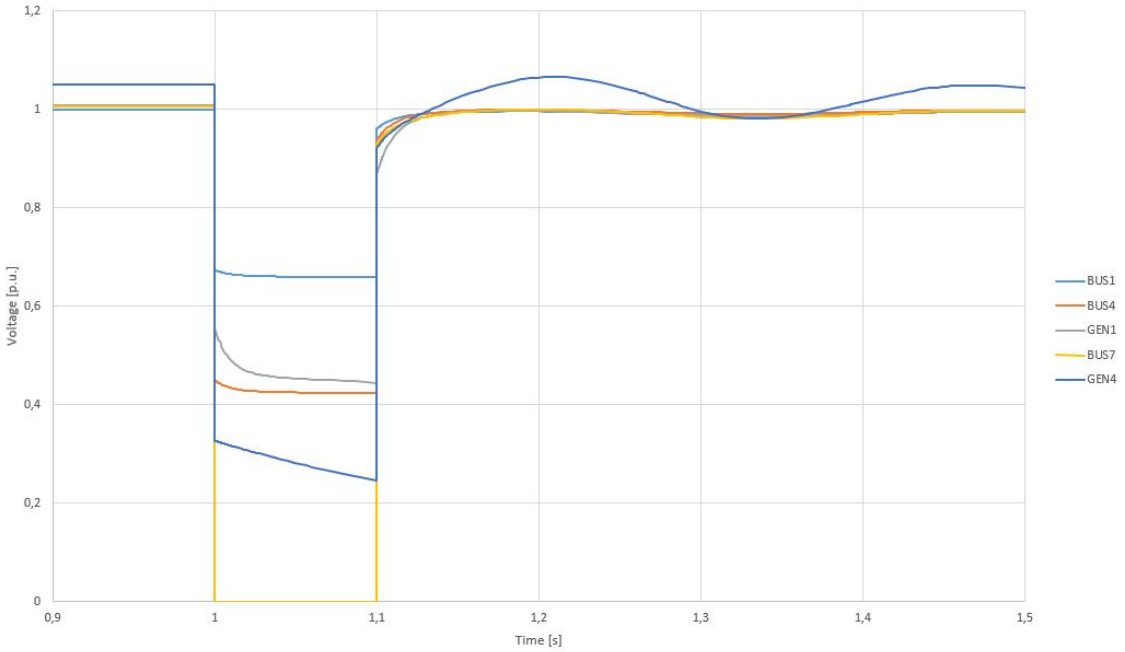

Figure 7.1: *Voltage magnitude responses after a 100 ms 3 phg fault at BUS 7*

As seen in figure 7.1, the nodes closest to the swing bus had the most stable voltage profiles. The voltage magnitudes decreased throughout the fault on all the nodes, but more rapidly

on the two nodes connected to the generators. The responses can be compared to the real faults seen in section 4.1. The real faults lead to almost square-shaped voltage dips with more stable voltage magnitudes. Studying the single line diagram of the Snåsa grid, the only thing between bus 4 and GEN1 is the transformer, modelled as an impedance. The voltage drop between node GEN1 and BUS4 may therefore be described as current times transformer reactance. The short circuit impedance seen from GEN1 will have a larger reactive component than BUS4, and that is why the voltage will drop more gradually. The voltage magnitude is lowest at bus GEN4, which is a node in the end of the radial. With a fault on BUS7, DG4 will be the only generating unit to feed the loads on the radial. The voltage will be reduced to be able to deliver enough power to the loads. The loads in dynpow were modelled as in equation (5.1), with MP equal to two. The voltage drop relative to the pre fault voltage would therefore lead to a relative power loss squared.

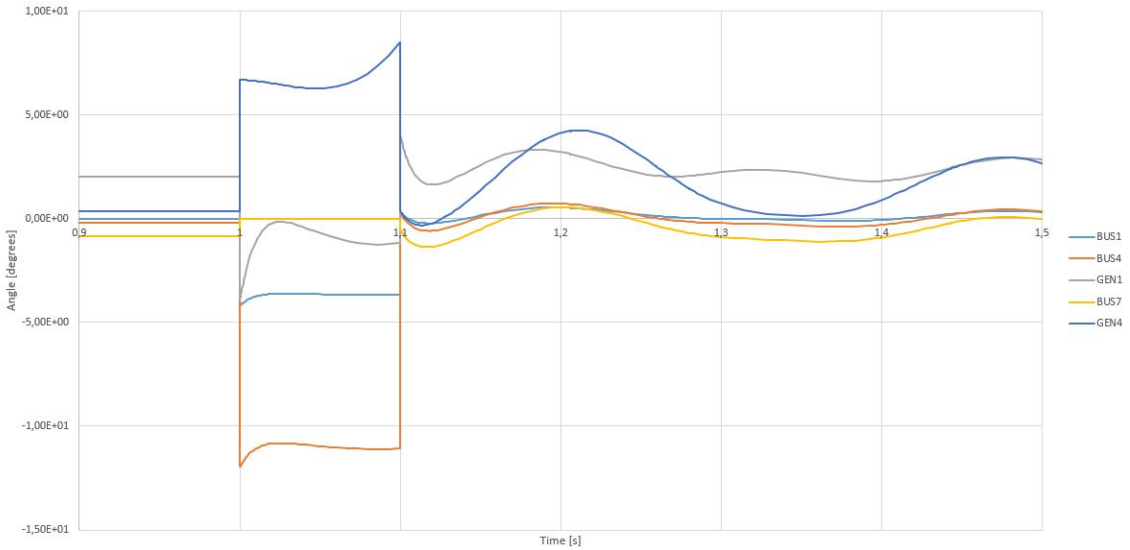

Figure 7.2: *Voltage angle responses after a 100 ms 3 phg fault at BUS 7*

The voltage angle response for the same fault is shown in figure 7.2. The response is seen to be largest on GEN4. When bus 7 was short circuited, generator DG4 had to cover all the loads from BUS7 and further down in the radial. Pre fault, a current was flowing from node BUS4, and further down the radial to feed power to the loads. Post fault, the point of operation changed rapidly seen from DG4, and the change in voltage angle can be explained by the reactive power demanded by the island-grid. The voltage angle on BUS 7 went to zero as the voltage went to zero, and the voltage angle above the fault changed in the opposite direction as the voltage angle on GEN4 because of the sudden surplus in reactive power.

Figure 7.3 shows the voltage angle on the terminals of DG1 with faults on different nodes. As seen in the figure, the voltage angle peaks were much higher when the fault occurred between the swing bus and the generator than when faults occurred in the parallel radial. That is because the swing bus will compensate for the fault, and when the DG units are in island mode, they will have to change their operating point to compensate for the missing swing bus generator.

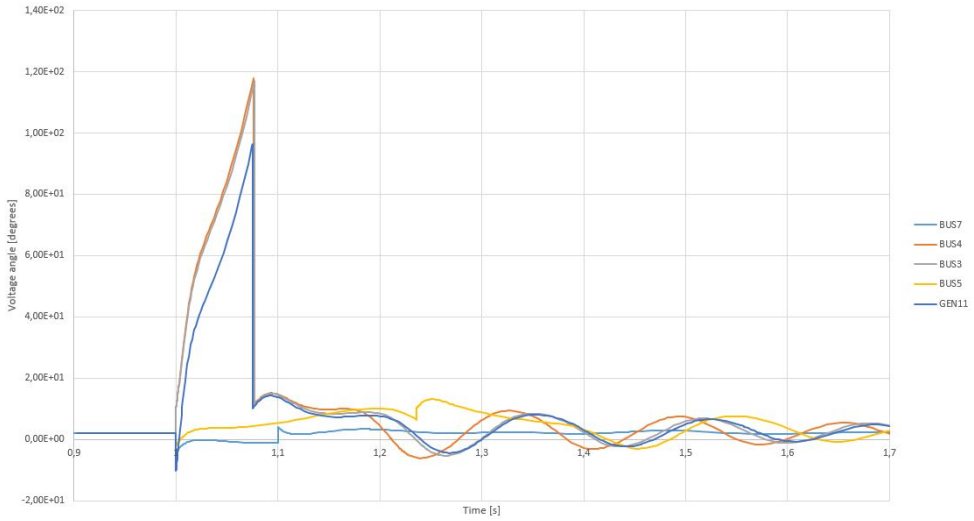

Figure 7.3: *Voltage angle on the terminals of DG1 (GEN11) when 3phg faults occur on different nodes*

7.1.2 Impact of Voltage Angle in Fault Ride Through Capability Assessment

To study the impact of voltage angle in FRT capability assessment, two cases were made. In case 1, a three phase fault was implemented on a node in the simulation model of the Snåsa grid. In case 2, the voltage magnitude from the generator terminals in case 1 was implemented on the same node. The result was the same voltage dip seen from the power plant, but the voltage angle was not affected to the same extent. This is seen in figure 7.4 which shows the simulated voltage angle for the two cases after a fault implemented at node BUS5.

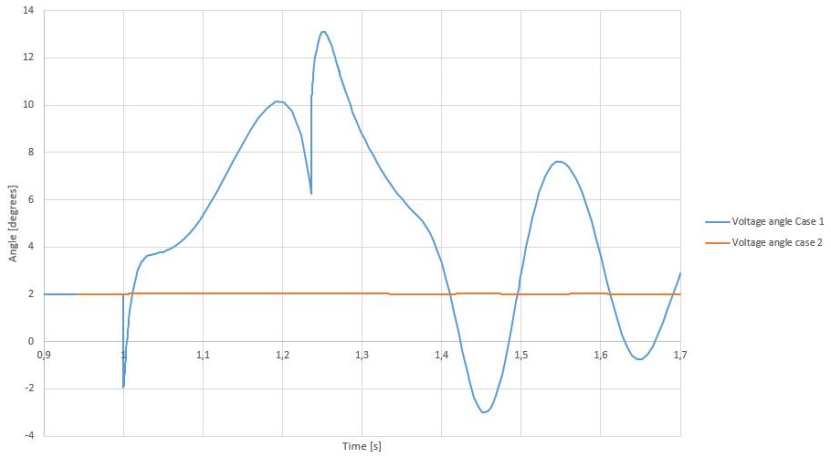

Figure 7.4: *Voltage phase angle compared to the swing bus at the generator terminals for Case 1 and Case 2 with a 236 ms fault on BUS5*

For all simulations, the VAr-regulator was used on the generator DG1 and the simple AVR was used on DG4. The critical clearing time for DG1 was simulated for the two different cases, and the results can be seen in table 7.1.

Table 7.1: *Critical clearing times for the two cases*

Node with fault	CCT Case 1	CCT Case 2	Increase [%]
BUS4	76 ms	92 ms	21.0%
BUS3	77 ms	92 ms	19.5 %
BUS5	236 ms	245 ms	3.8 %
GEN11	75 ms	73 ms	-2.7 %

As seen, the critical clearing time increased for all nodes except one when the fault occurred on the generator node. The increase was largest for the faults happening between the generator and the swing bus. Figure 7.3 shows that the voltage angle change was largest during those faults. This verifies the hypothesis that the voltage angle has a large impact on the FRT capability.

There is one result that deviates from the norm. That is the fault where the generator terminals were completely short circuited. Studies of fast decoupled load flow emphasize the strong connection between voltage level and reactive power. As seen in figure 7.5, the field voltage reached saturation, and increased the transmitted reactive power, seen in figure7.6. The generator stayed over-magnetized even when the fault was cleared and the voltage went back to the original state. To troubleshoot the system, all the dynamic parts of the grid were removed to see whether they influenced the response, but no relation was seen. The problem seemed to be in the voltage regulator, and the simple AVR was therefore used for the same test. The result was a more proper field voltage, seen in figure 7.7. With the simple AVR, the clearing time for case 1 was 75 ms as before, and it increased with 1 ms for case 2.

The increase in clearing time was not as extensive for the fault on the terminals of the generator compared to the other faults with origin between the swing bus and the DG unit. Since the increase in reactive power is related to the rotor angle, theta had to increase to be able to deliver the demanded reactive power. The generator lost synchronism when reaching 180°. A difference has been seen between the a fault on BUS4 and a fault on the generator terminals, where the only thing separating the nodes is a line and a transformer. The inductances consume reactive power, and seem to be an important component in this study. This may be a topic for further studies.

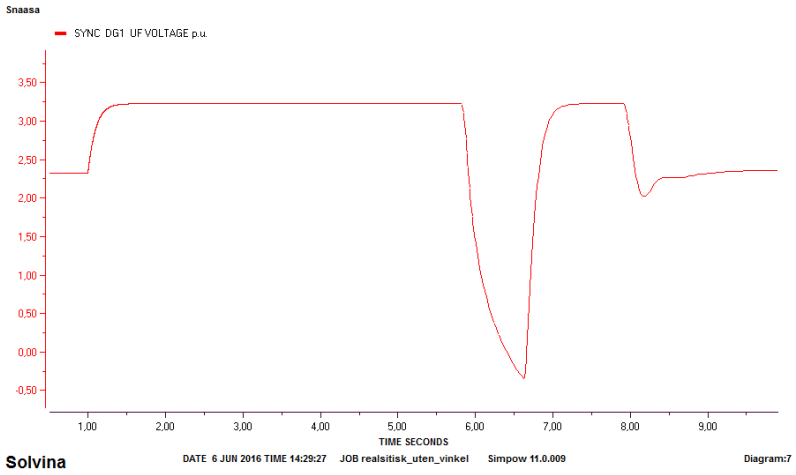

Figure 7.5: *Field voltage during Case 2, fault implemented on the terminals of the generator. VAr-regulating mode.*

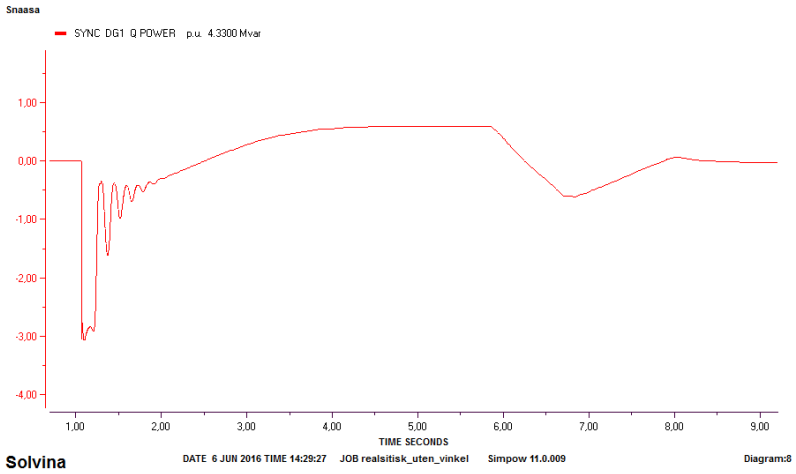

Figure 7.6: *Reactive power delivered from the generator during Case 2, fault implemented on the terminals of the generator. VAr-regulating mode.*

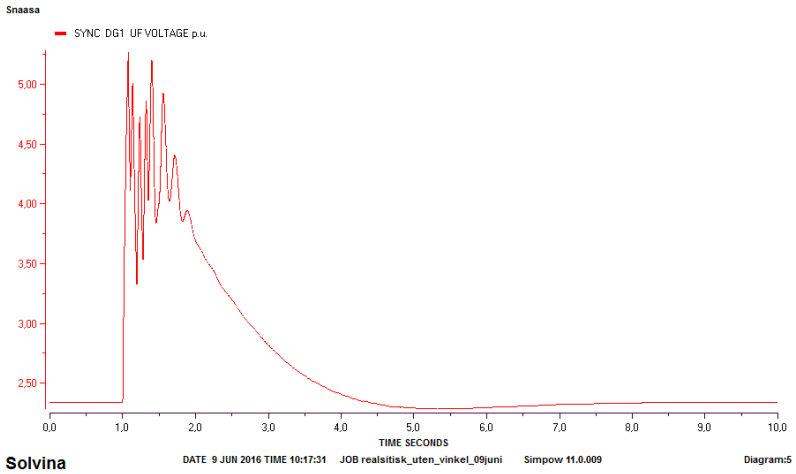

Figure 7.7: *Field voltage for case 2 with the simple AVR, without reactive power regulation*

7.2 DipLab Field Experiments

SINTEF Energy Research made experiments with the DipLab the 13th and 14th of April 2016. The tests were made at Bruvollelva Power Plant, in Snåsa, Nord-Trønderlag. The production in the power plant was fluctuating about 2 MW both days, with about 200 kW variation. In total five test were done, but the measuring tool Elspec did not log more than three of the tests successfully. There was also an oscilloscope connected, but one of the tests was not logged with the oscilloscope either. The five tests are listed in table 7.2, along with the result "Trip" or "No trip". The column called "Theoretical dip" describes the pre calculated depth of the voltage dip. X_{sr} and X_{sc} describes the series- and parallel reactances, while "Time" describes the duration of the dip, meaning the time from the shunt break was closed until it was opened again. The parallel reactance was included to the circuit about 10 seconds before the series reactance, and was removed one second after the dip. The measuring equipment was placed between the lab and the transformer, on the 22 kV grid.

Table 7.2: *Test Plan*

Test number	Theoretical dip [%]	X_{sr} [Ω]	X_{sc} [Ω]	Time [ms]	Regulator mode	Result
1	20 %	32.95	144.15	500	cosϕ	No trip
2	20 %	32.95	144.15	3000	cosϕ	Trip
3	20 %	32.95	144.15	200	AVR	No trip
4	30 %	32.95	85.58	200	AVR	Trip
5	30 %	32.95	85.58	100	cosϕ	No trip

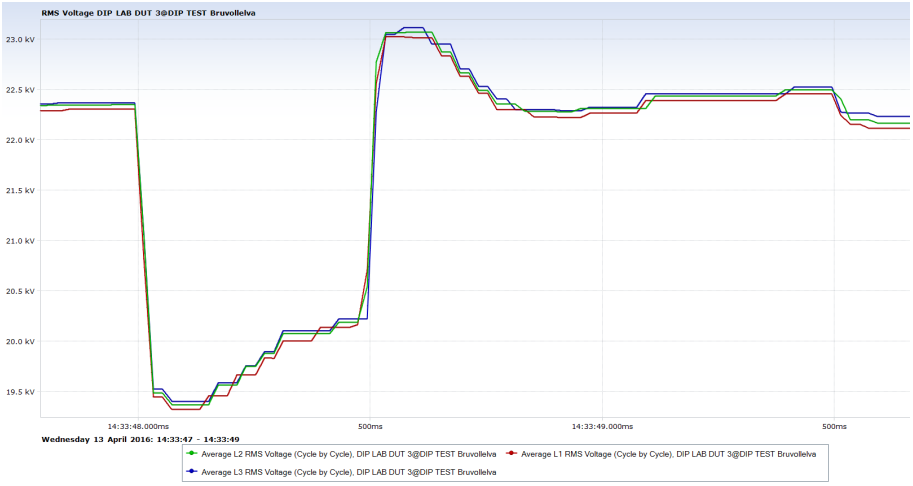

Figure 7.8: *Terminal voltage logged during test 1*
Source: *[1]*

Figure 7.8 shows the voltage dip during test number 1. The voltage decreased immediately to about 19.4 kV, which corresponds to about 87 % of the voltage pre fault. After that, the voltage increased slowly to about 20.2 kV, probably caused by the voltage regulator, which had sensed the voltage decrease and compensated by an increase in the

magnetization current. When the short circuit reactance was disconnected, the voltage increased momentarily, and reached 23 kV. The voltage level was higher than the nominal voltage because of the magnetization level. When the AVR sensed that the voltage was too high, a signal was sent to the exciter, and the field voltage was reduced. The terminal voltage went back to the same state as before the voltage dip.

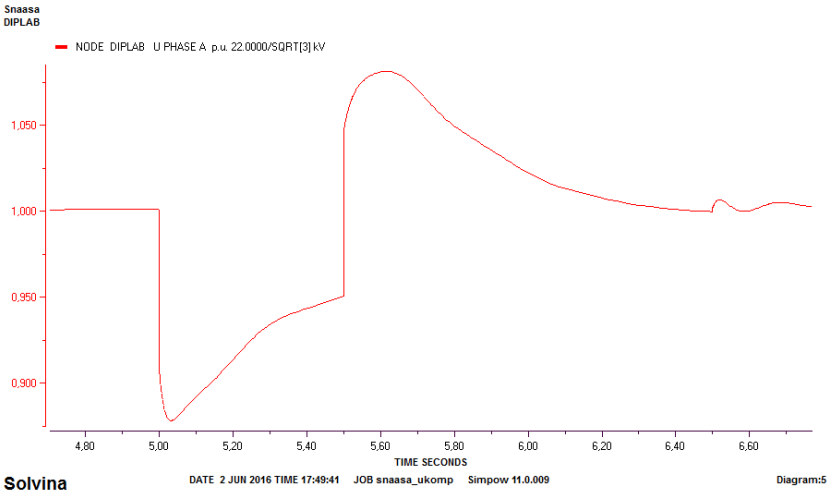

Figure 7.9: *Simulated terminal voltage for test 1 with P=2MW, Q=0MVAr*

The same test was simulated in figure 7.9. The series reactance was included at time 1 second, and the switch connecting the short circuit reactance was closed four seconds later. As in the physical lab, the series reactance was disconnected one second after the voltage dip was cleared, by closing the switch in the parallel line. The shape of the simulated voltage dip was almost the same as the measured, as the voltage increased until the voltage regulator reached the saturation limit. The minimum voltage magnitude in the simulated voltage dip was 0.88 per unit, which is almost the same as in the measured dip, which approached 87 %. One difference between the two plots is how fast the voltage dropped. The voltage dropped linearly in the real life test, while the simulated voltage had an instant drop, before the rate slowed down.

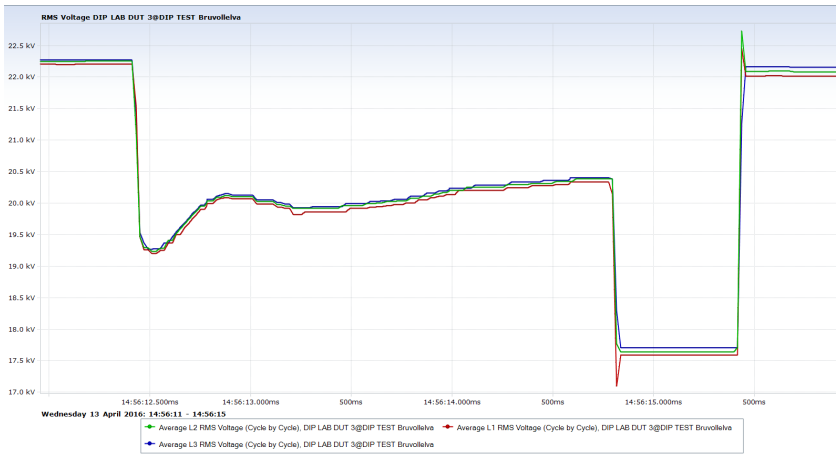

Figure 7.10: *Terminal voltage during test 2*
Source: *[1]*

Figure 7.10 shows the voltage dip during test 2. The voltage decreased fast as the short circuit reactance was connected. The voltage increased slowly, because of the the voltage regulator. As the field voltage reached its limit, the voltage stabilized until the generator tripped. The trip happened after approximately 2.5 seconds, when the voltage dropped to about 17.6 kV. The cause of the trip is unknown, as there were no alarm messages on the screen inside the power station. The most probable cause is that an under voltage protection relay sensed the voltage dip, causing a disconnection between the generator and the grid. The under voltage relay ANSI 27 described in appendix A.3 should disconnect the generator from the grid if the voltage dip is below 0.9 per unit for more than 1.4 seconds. A probable explanation is that this protection unit tripped the power plant.

To explain the voltage profile in more detail, it is necessary to understand what happened in the system during the dip. The current was in the beginning flowing from the generator, feeding both the series inductance and the short circuit inductance. When the generator was disconnected, the current through the series reactance changed direction as the surrounding grid was the only unit feeding the short circuit. The voltage changed instantly, and became a result of voltage division between the series- and short circuit inductances. By assuming 1 p.u voltage on the grid side of the series reactance, the voltage in the measuring point became as in equation (7.1). Three seconds after the dip was started, CB2 was disconnected, and the short circuit reactance was removed. The current had no path, and the voltage drop was zero over the series reactance. The voltage was therefore the same as the grid voltage for the final part of the plot.

$$V_{measured} = V_{grid}\frac{X_{sc}}{X_{sc} + X_{xr}} = 1.p.u.\frac{144.15}{144.15 + 32.95} = 0.814p.u = 17.9kV \tag{7.1}$$

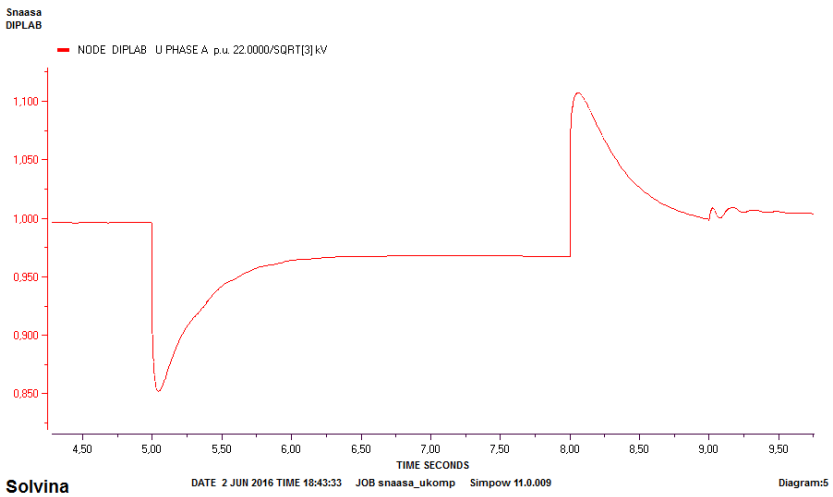

Figure 7.11: *Simulated terminal voltage for test 2 with P=2MW, Q=0MVAr*

Figure 7.11 shows a simulation of test 2, and can be compared to the plot in figure 7.10. The depth of the simulated and measured voltage dips were approximately equal. Both voltage dips increased slowly, because of the work of the excitation system. A difference can be seen in the two plots as the voltage increased more in the simulated voltage dip than in the real dip. The reason was probably the field voltage limit, which seem to be

too high in the simulation model. That can also explain the size of the overshoot when the fault is cleared. The protection relays were not implemented in the simulation model, and that is the reason why the generator tripped in the real test, but not in the simulated model.

The two experiments made with the simple AVR without the additional PF-mode gave results similar to the ones made with PF-mode. The oscilloscope plot from test number 4 can be seen in figure 7.12. The plot can be compared to figure 7.13, which is the oscilloscope plot from test number 5. Both dips had the same reactance configurations, but test number 5 had a duration of 100 ms instead of 200 ms.

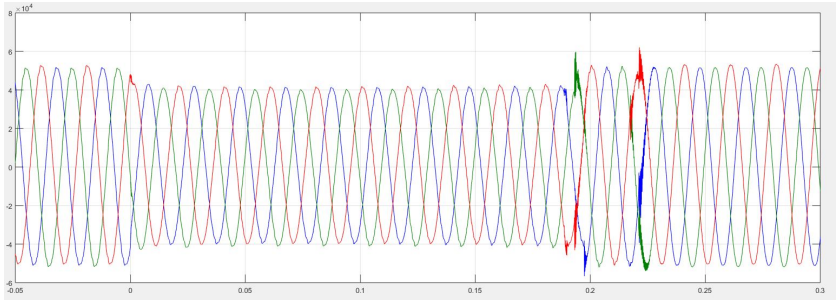

Figure 7.12: *Terminal voltage during test 4*
Source: *[1]*

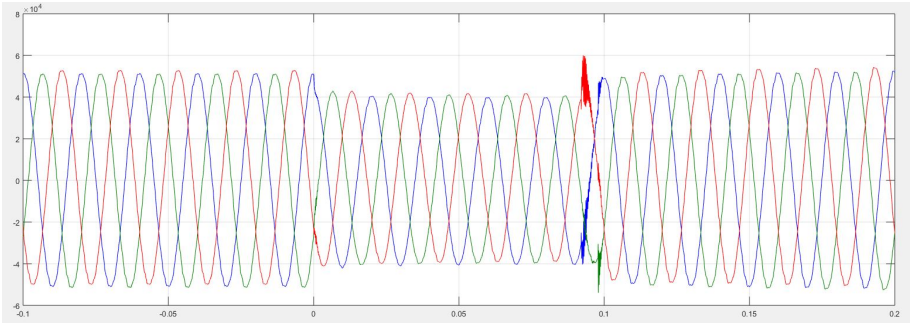

Figure 7.13: *Terminal voltage during test 5*
Source: *[1]*

As seen in the two plots, the voltage dips seemed to be quite similar with the different regulator modes. This was expected, as the main part of the regulatings are the same for the two modes, and the only difference is the additional loop implemented with a large time constants. The quick response is therefore the same, while the PF-loop will work slower.

Figure 7.14 and 7.15 show the same dip as in figure 7.13, logged with the Elspec. The reactance configuration was changed for the two final tests, which resulted in a voltage dip of approximately 21%. As seen in figure 7.14, the same overshoot as seen in the earlier test happened when the dip was cleared, but the voltage was soon to be adjusted back to normal. The response was quite similar to the simulated voltage dip, seen in figure 7.17. Figure 7.15 shows the shape of the dip in more detail, and may be compared to

the simulated dip in figure 7.17. The real dip did not have the same initial change as the simulated dip, and the voltage regulator on the real generator was capable of keeping the voltage more stable throughout the dip, making the dip more square-shaped. The initial voltage drop is clearly not as instant in the real world compared to simulations.

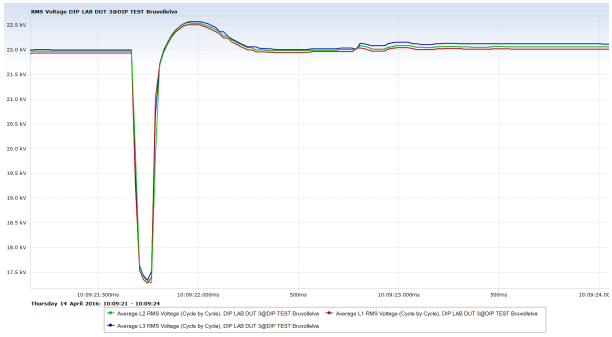

Figure 7.14: *Terminal voltage, test 5 [1]*

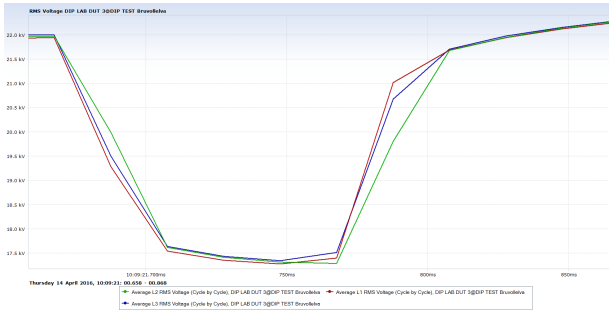

Figure 7.15: *Terminal voltage, test 5 [1]*

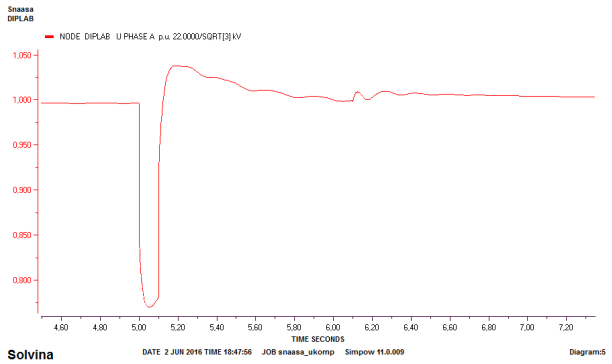

Figure 7.16: *Simulated terminal voltage for test 5 with P=2MW, Q=0MVAr*

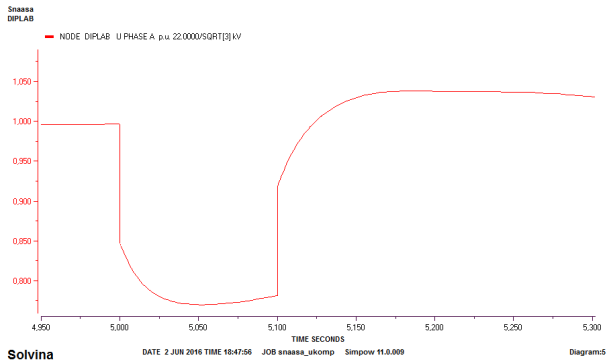

Figure 7.17: *Simulated terminal voltage for test 5 with P=2MW, Q=0MVAr*

The depth of the voltage dip was highly dependent on the power drawn from the generator. This can be seen in figure 7.18, where the voltage dip resulting from test 1 was simulated with a power of 1, 2, 3 and 3.9 MW produced by DG1. A higher production leads to a higher current, and hence a higher voltage drop.

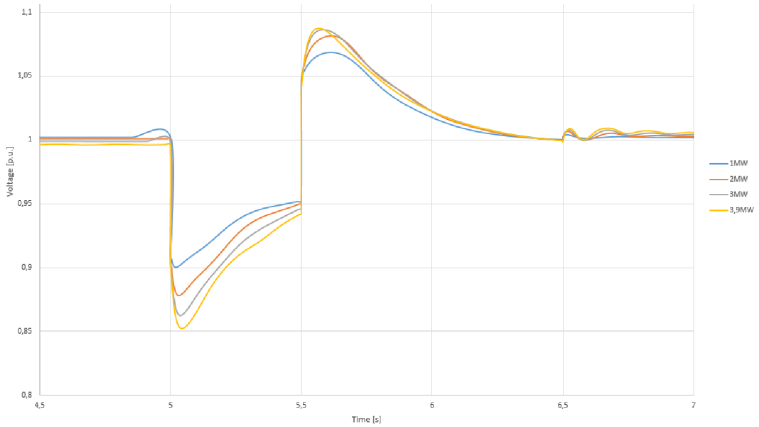

Figure 7.18: *Test 1 simulated with four different productions on DG1*

8 | Results - In-House Lab

The in-house lab had a synchronous generator driven by a permanent magnet motor. An inductance was placed between the generator and the grid. A signal generator controlled an electronic three phase relay, connecting and disconnecting a short circuit inductance.

8.1 Case 1: Strong Grid Connection

Multiple tests were done to look into the FRT capability of the machine. The size of the inductances were not possible to change with the equipment available, and the torque was therefore adjusted instead. The tests with accompanying results (Trip or No trip) are listed in table 8.1. Only one of the tests resulted in a generator trip in the laboratory experiment. The same tests were simulated in SIMPOW. The torque was modelled as produced power in the optimal power flow calculation, where the power was calculated by equation (6.3). The maximum torque used in the tests was 7 Nm, which corresponds to 1.1 kW, and 1.1 per unit. The results from the experiments and from the simulations were quite different, which can be seen in the right column of the same table.

Table 8.1: *Test Plan for the in-house lab*

Test number	Dip duration [ms]	Torque [Nm]	Result lab	Results simulations
1	100	0	No trip	No trip
2	100	-1	No trip	No trip
3	100	-2	No trip	No trip
4	100	-7	No trip	Trip
5	200	0	No trip	No trip
6	500	0	No trip	No trip
7	500	-7	Trip	No trip
8	200	-7	No trip	Trip
9	300	-7	No trip	Trip
10	400	-7	No trip	Trip
11	450	-7	No trip	Trip
12	500	-7	No trip	Trip

Generally, the simulation model made the generator trip before the laboratory model. The critical clearing time for the different torques were simulated, and the results can be seen in table 8.2, and plotted in figure 8.1.

Table 8.2: *Simulated critical clearing time for different values of torque*

Torque [Nm]	CCT [ms]
0	infinite
-1	infinite
-2	infinite
-3	infinite
-4	161
-5	117
-6	93
-7	77

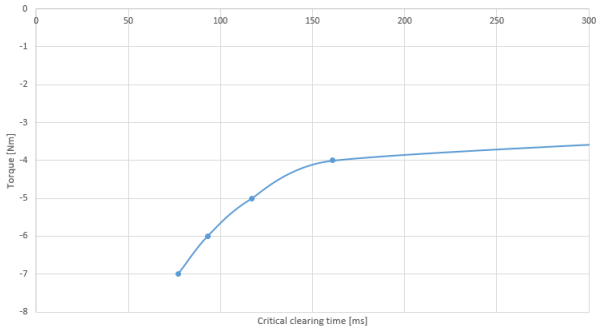

Figure 8.1: *Simulated critical clearing time as a function of torque*

The results from the lab was then plotted along with the simulated curve. The red dot shows the test that lead to a generator trip, while the green dots are used where the generator did not trip. The figure can be seen in 8.2. In the simulations, all the dots below the blue line lead to a generator trip, while all the dots above kept the generator in a synchronous mode. As seen, this is not the case for the experimental results. Almost all the dots below the blue line are green, and not red as in the simulations.

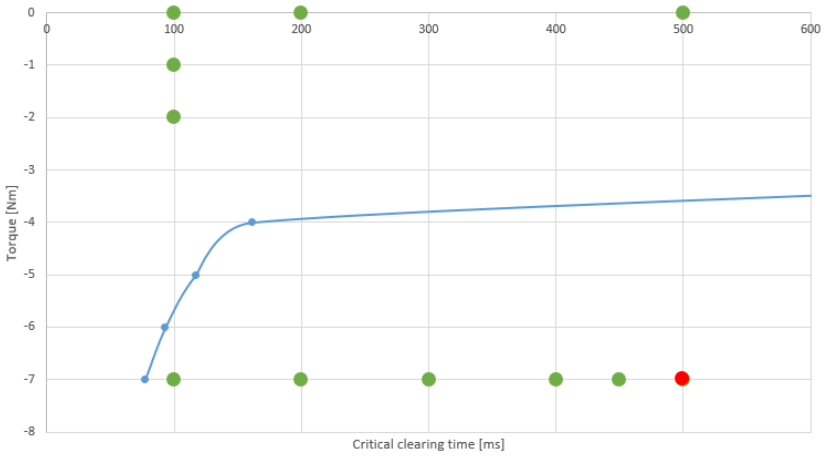

Figure 8.2: *Simulated critical clearing time as a function of torque and test results from the lab plotted together. Red equals trip, green equals no trip*

Figure 8.2 shows some major differences between the critical clearing time for simulations and for laboratory testing. The voltage profiles for the different tests were plotted, and figure 8.3 shows the terminal voltage measured during test 1. The plot may be compared to the simulated voltage dip in figure 8.4

As seen in the two figures, the voltage dropped faster in the simulated dip than in the

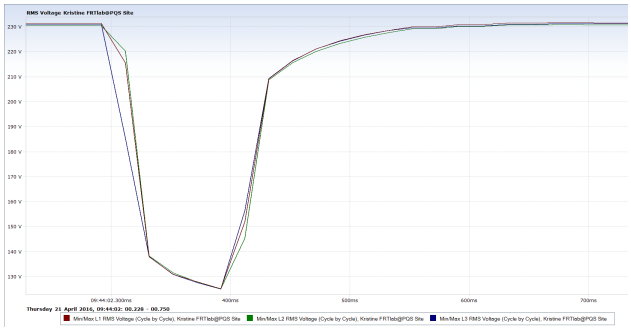

Figure 8.3: *Terminal voltage during test 1*

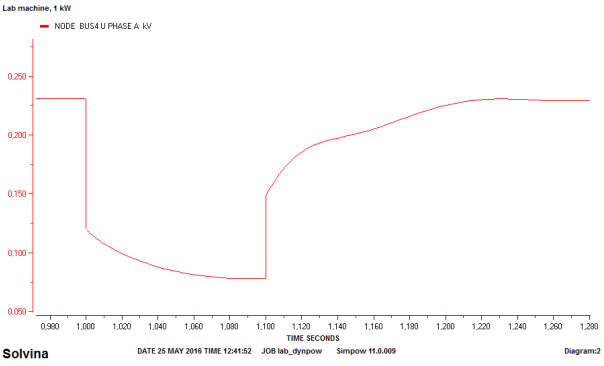

Figure 8.4: *Simulated terminal voltage during test 1*

physical. The instant voltage drop was also deeper in the simulations, as the voltage dropped instantly to 120 V and then slowly approached 75 V while the lab results showed a voltage dip instantly down to 138 V, and then slowly approaching 125 V. The difference in critical clearing time as a function of torque may therefore be a result of a difference in voltage dip magnitudes. There are many possible reasons for why the simulated voltage dips deviated from the measured dips. First, the simulation model was based on a larger and more complex machine operating in a real grid, and the lab machine may not be designed to fit into the same simulation model. Secondly, the parameters used in the simulations include uncertainties as they were measured, and not found in a data sheet. Finally, as seen in figure 7.18, the power drawn from the generator has a large impact on the voltage dip magnitude, and the power should therefore have been measured to make sure that the simulations were made with the same power.

Figure 8.5 shows the plotted voltage for test 7, which was the test leading to a generator trip. As seen, the voltage oscillated for a while before the emergency stop button was pushed, removing all electrical power from the system. The oscillations show that the generator lost the synchronism to the main grid, and struggled to find a stable operating point.

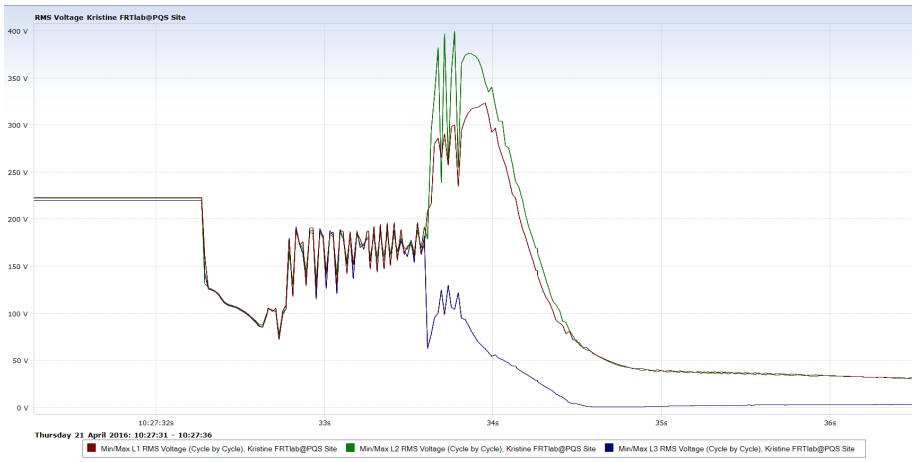

Figure 8.5: *Terminal voltage during test 7. The generator tripped.*

8.2 Case 2: Weak Grid Connection

For case 2, a three phase cable was placed between the grid and the series reactance to make the grid weaker. Simulations show that the critical clearing time was slightly lower with the cable implemented. This is seen in table 8.3. The decrease in clearing time was so small, no difference were expected in the lab experiments either.

Table 8.3: *Simulated critical clearing time for different values of torques with and without the additional cable*

Torque [Nm]	CCT without cable [ms]	CCT with cable [ms]
0	Infinite	Infinite
-1	Infinite	Infinite
-2	Infinite	Infinite
-3	Infinite	Infinite
-4	161	161
-5	117	117
-6	93	91
-7	77	77

The generator was tested two times at 7 Nm and 500 ms duration without cable, and one of the tests resulted in a loss of synchronism, while the other did not. A generator trip was therefore expected when testing the same torque and duration with the cable. Table 8.4 shows the tests that was made with the additional cable. Surprisingly, the additional cable made the clearing time longer, and the machine did not trip until the dip lasted for 600 ms.

Table 8.4: *Test Plan with additional cable to make the grid weaker*

Test number	Dip duration [ms]	Torque [Nm]	Result
13	450	-7	No trip
14	500	-7	No trip
15	500	-7	No trip
16	520	-7	No trip
17	550	-7	No trip
18	575	-7	No trip
19	600	-7	Trip

The voltage dip during test 14 can be seen in figure 8.6. The voltage oscillated for a short while. It was apparent that the machine was struggling, as it made a lot of noise. When the fault was cleared, the machine managed to get back on the grid. The result was surprising, as the rotor angle in a weak grid has a higher initial point of operation, which makes it more likely to reach the stability limit of 180° during a fault. From the

results, it seem like that the inductance separates the generator from the grid in a positive way. The machine looses synchronism, and starts slipping, but manages to get back in synchronous mode when the fault is cleared.

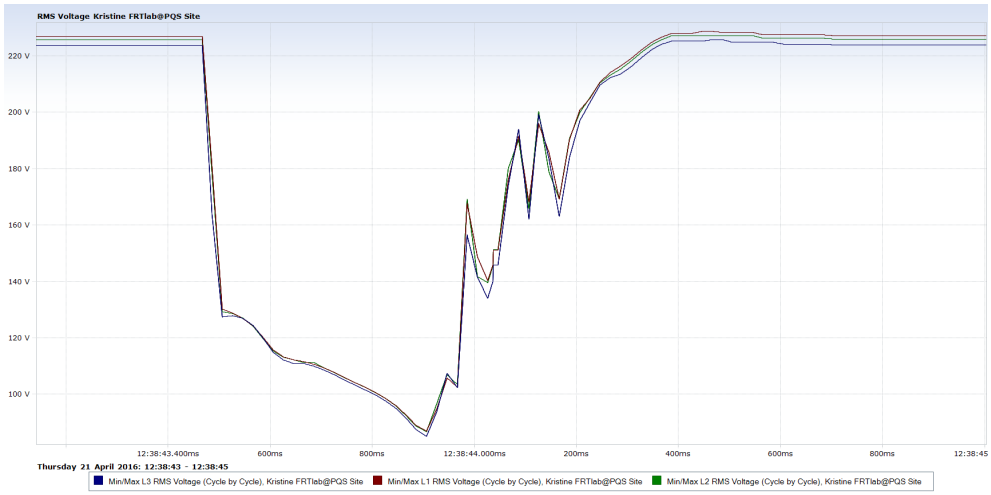

Figure 8.6: *Terminal voltage during test 14*

Figure 8.7 shows the results from test 19, where the generator tripped. The voltage slipped the same way as in 8.6, but the generator did not manage to get back in synchronism, and the emergency stop had to be pushed.

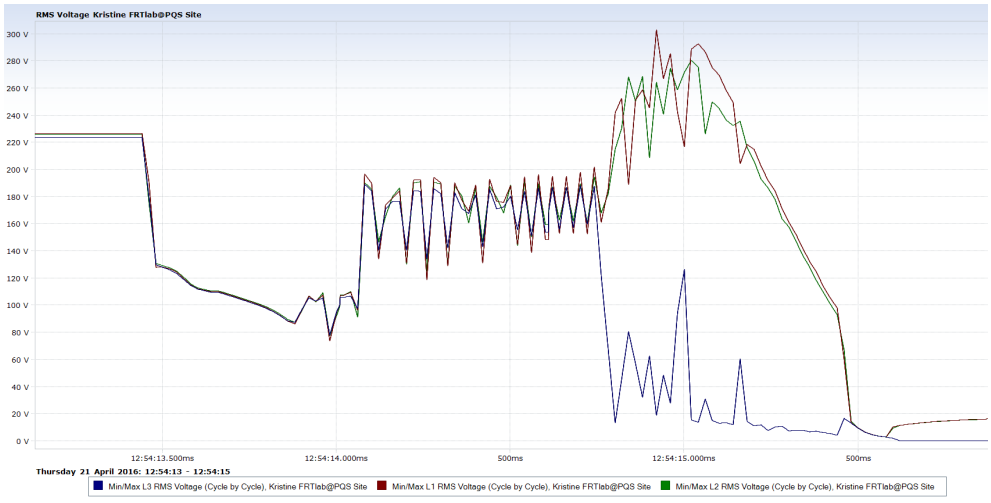

Figure 8.7: *Terminal voltage during test 19*

9 | Discussion

By studying the data of transient faults in the Norwegian grid, three phase short circuits seem to be a common cause of voltage dips in the distribution grid. The voltages are equal in all phases. Three phase to ground faults seem to be a good design condition for restrictions regarding voltage dips.

As seen in chapter 7.1, both voltage magnitudes and voltage phase angles are changed in the entire system during at three phase fault. The magnitudes are dependent on the short circuit impedances between the node and the faulted node. During the computer simulations, the voltage magnitude on the swing bus was the most stable, and the voltage dips had the lowest magnitudes when the DG units became disconnected from the swing bus. The voltage angle also had the highest peaks in the same cases, where the DG units had to cover the loads, and the point of operation therefore changed the most.

When studying the critical clearing time for a realistic fault compared to a voltage dip without the same change in voltage angle, the clearing time increased with up to 20%. The largest increase in clearing time was seen when the faults were simulated on a node between the DG-unit studied and the swing bus. In other words, the voltage angle impact was most severe in the cases where the voltage angle increased the most, making the fault ride through capability assessment highly dependent on the voltage angle. As seen in table 7.1, the difference in critical clearing time was not more than 3.8% when the fault was placed on node BUS5, which is further down in the radial. This made sense, as the change in voltage angle was small during the realistic fault. The central- and regional grid is organized differently than the distribution grid. The severity of a disconnected line is larger, and the n-1 rule stating that the system should be able to operate stably even with a severe contingency should be obeyed. A generating unit connected to the higher voltage levels will therefore always be connected in a meshed grid, making the island mode almost impossible. The voltage angle peaks will therefore never be as large in the higher voltage levels as in the radials in the distribution grids. The importance of including voltage angle as a part of the fault ride through capability assessment may therefore be more relevant for the distributed generation units.

The implementation guidelines for network codes "Requirements for Grid connection Applicable to all Generators"[26] states the importance of short-circuit capacity at the connection point in the pre-fault and post-fault condition. The short-circuit capacity represents the robustness of the network, and has a significant impact of the FRT performance. It should therefore be taken into proper consideration when specifying the requirements.

> *System characteristics like network topology and generation mix have significant impact on the relevant parameters of the fault-ride-through requirement and should be taken into account reasonably by the relevant network operator when selecting them.*[26]

To verify the voltage angle impact on the critical clearing time of a synchronous generator, a small scale lab was built. Dips were made by use of a short circuit reactance. The lab machine may differ from the larger machines operating in the power grid, as the intentions of use are completely different. The design parameters may therefore differ from those in a larger machine. There are many uncertainties when it comes to the design parameters of the lab machine. No data sheets were obtained, and the simulation parameters were decided through tests and measurements on the machine. The cable used to create a weaker grid were shorter than intended, making the impact in voltage angle small. In spite of this, the results from the experiments were clear, as the cable made the critical clearing time longer, and not shorter as presupposed. The test with 7 Nm torque and 500 ms dip made the generator trip one out of two times. To make sure that the trip was not just a coincident, more tests should have been made, but it was chosen to stop because of wear on the equipment. Another factor that may have influenced the in-house lab results was the temperature on the generator. Multiple tests were made with short intervals, making the generator warm due to high currents. This may have influenced the performance of the machine.

Another problem with the in-house lab was that the prime mover was connected to the same grid as the generator. The prime mover power supply experienced the voltage dip, and that may have influenced the results. The reason for this setup was because it was advantageous for the whole system to respond to the same emergency stop switch button.

The DipLab results can be useful for two things in particular. That is to study the FRT capability of the generating unit, and to compare the results to simulations to evaluate the accuracy of the simulation results. The experiments made at Bruvollelva was not sufficient to evaluate a FRT characteristic. The generator trips were caused by protective relays, and not by out of step behaviour in the generator. Protection relays should therefore be added to the simulation results. It is the FRT capability of the whole generating facility that is being considered in the FRT requirements, and the settings of the protection relays are therefore important to take into account. Protection relays are present to protect the grid, the generator and other parts of the production unit. To maintain a stable grid, it is therefore important for all parties to have a well protected machine.

Experiences can be drawn from the voltage dips registered at Snåsa. The shape of the measured voltage dips were quite similar to the simulated dips. What differed the most was that the voltage did not change as instant in the real world as in the simulation model. Another observation from the results was that the voltage dips simulated with a low generator production gave much shallower dips than with a higher production. This is important to have in mind when simulating short circuits. Results from DipLab test 2 showed that the voltage dip stabilized at a lower voltage level in the real world than in the simulations. The field voltage limitation should therefore have been reduced in the simulation model for more realistic results. The same thing is seen in the overshoots

occurring after the fault has been cleared.

The dips caused by the DipLab were more square shaped than the simulated dips. This is especially seen in the plots from test 5, simulated in figure 7.14. The real voltage disturbances seen in section 4.1 had approximatly the same shape as seen in the DipLab tests. Figure 7.1 showed though that the voltages at the generator nodes were less square shaped than in the rest of the system, because of the inductances in the generator and in the generator transformer, creating a more inductive short circuit impedance. Figure 7.18 showed that the larger power produced from the generator, the deeper initial voltage dips, and the larger deviation from the square shaped dip. This should be considered as disturbances tend to happen during heavy load periods.

10 | Conclusion

When studying the voltage dips caused by three phase symmetrical faults in the distribution grid, the location of the fault has proven to be important. The voltage dips with origin in a fault in a parallel radial to the point of measurement gives a small fluctuation in voltage angle, while faults between the point of measurement and the swing bus creates larger changes in voltage angle. The reason is that the whole load flow changes when the swing bus is disconnected, and the DG units have to cover all the demand. As the current increases during a fault, so does the losses in the lines. As the lines are mainly inductive, the voltage angle will change for the generator to be able to supply the system with the reactive power demand.

The critical clearing time of the distributed generating unit Bruvollelva was simulated in this report for two different cases. In case 1, three phase symmetrical faults were simulated on different nodes in the Snåsa grid model, and the critical clearing time was found by checking how long the fault could last before the generator got out of step. The voltage magnitude on the generator terminals from case 1 was saved, and implemented on the same node for case 2. The voltage magnitudes seen from the generator was therefore the same for the two cases, but the voltage angle did not have the same response in case 2. The voltage magnitude was then changed by increasing the length of the dip until the critical clearing time was reached. The increase in critical clearing time was about 20% for the voltage dips with origin between the DG unit and the swing bus, while the increase was much lower for the faults with origin in a parallel radial. A correlation can be seen, as the faults leading to the highest fluctuations in voltage angle was the same faults that gave the largest increases in clearing time. This indicates that the voltage angle has a considerable impact on the critical clearing times of the machine, and hence a considerable impact on the fault ride through capability assessment.

The results emphasize the importance of including voltage angle as a part of the fault ride through capability assessment, and especially for DG units, as they usually are placed in weaker grids with a lower short circuit capacities. The implementation guidelines for network codes amplifies the importance of the short-circuit capacity at the connection point in the pre-fault and post-fault condition. The robustness of the network has significant impact of the FRT performance, and a minimum requirement for short circuit capacity should be defined in the national FRT restrictions.

An in-house lab was built to verify the results from the simulations. The outcome was surprising, as a weaker grid connection lead to a clearing time of 600 ms when the generator

was operating at 7 Nm, while the stronger grid connection made the generator trip at 500 ms. The experiments should have been made with a longer cable, and should be repeated for more credible results.

Another verification of the simulation model was made when the measurements from the experiments made at Bruvollelva was compared to the simulations. The results showed that the voltage dips were similar, but protection relays should have been implemented to the simulations model, as they were a limiting factor when it came to the clearing time of the fault.

Generally, the measured dips caused by the DipLab were more square shaped than the simulated dips. The real voltage disturbances seen in section 4.1 were also quite square shaped. Figure 7.1 showed that the voltage due to a three phase fault had a large initial dip at the generator nodes as in the rest of the system due to a higher inductance in the short circuit impedance. This is especially the case for periods with high production. That is seen in figure 7.18.

To sum up, there are especially two things that should be taken into consideration when choosing the grid codes concerning the DG units. First of all, the voltage angle fluctuations have a large influence on the critical clearing time, and should therefore be emphasized as a part of the grid codes. Secondly, the initial part of the voltage dip at the generator terminals may be deeper than the rest of the dip, and the shape of the dip is not the same at the generator terminals as in the rest of the grid. This is especially the case when the production is high. As trees are more likely to fall during heavy load periods, and production are increased during heavy rain and bad weather, the problem should be considered.

11 | Further Work

To improve the knowledge and understanding of this topic, further studies are recommended to include some of the following work:

- From the DipLab results at Snåsa, protective relays have proved to be important when deciding the critical clearing time. In further studies, these relays should be implemented to the simulation model to see if they behave as expected.
- The voltage regulator seemed to have a larger field voltage limit in the simulations than in the real world. This should therefore be reduced in further studies.
- The case with a short circuit on the generator terminals presented in section 7.1.2 gave some surprising results as the clearing time was approximately the same with and without the influence of the voltage angle. This case should be studied in further detail.
- The in-house lab experiment gave some surprising results. To verify these, the following elements should be considered:
  - A larger quantity of results should be carried out to improve the credibility of the results
  - A longer cable should be used to make the difference between the two cases easier to observe
  - The depth of the voltage dip should be varied by changing the size of the short circuit inductance.
  - The power should have been measured to make sure that the power in the simulations and in the lab are equal
  - The experiments are mainly done with either a low or a high torque from the prime mover. The tests should also be made with a medium torque, such as 4, 5 or 6 Nm.

Bibliography

[1] Henrik Kirkeby. Sintef energi, testing av småkraftverks frt-egenskaper, 2016.

[2] Kristine Mamen Antonsen. Low voltage fault ride through capability in mini-hydro power plants - modelling and simulations of bruvollelva kraftverk, 2015.

[3] SINTEF Energi. *DIP TEST Prosjektbeskrivelse*, 2014.

[4] Fact sheet: General information about simpow. `http://www.solvina.se/wp-content/uploads/2015/01/General-info-about-Simpow3.pdf`. Accessed: 2016-05-30.

[5] The European Comission. *REGULATIONS - COMMISSION REGULATION (EU) 2016/631*, 2016.

[6] Tilknytningskodene: Rfg, dcc, hvdc. `https://www.nve.no/elmarkedstilsynet-marked-og-monopol/europeisk-regelverksutvikling/nettkoder/tilknytningskodene-rfg-dcc-hvdc/`. Accessed: 2016-06-04.

[7] IEC. *EN560*, 2010.

[8] Statnett SF. *Funksjonskrav i Kraftsystemet*, 2012.

[9] Prabha Kundur. *Power System Stability and control*. 2006.

[10] P. Kundur, J. Paserba, V. Ajjarapu, G. Andersson, A. Bose, C. Canizares, N. Hatziargyriou, D. Hill, A. Stankovic, C. Taylor, T. Van Cutsem, and V. Vittal. Definition and classification of power system stability ieee/cigre joint task force on stability terms and definitions. *IEEE Transactions on Power Systems*, 2004.

[11] Jan Machowski, Janusz W. Bialek, and James Richard Bumby. *Power system dynamics : stability and control*. John Wiley and Sons, Ltd, 2008.

[12] Stephen Chapman. *Electric Machinery Fundamentals*. 2012.

[13] Basler Electric. *DECS-200 Digital Excitation System - Instruction manual*, 2012.

[14] Peter Sauer and M.A. Pai. *Power System Dynamics And Stability*. Prentice-Hall, 1998.

[15] W. D. Stevenson JR. J. J. Grainger. *Power System Analysis*. McGraw-Hill International Editions, 1994.

[16] Thomas J. Domin J. Lewis Blackburn. *Protective Relaying, Principles and Applications*. CRC Press, 2007.

[17] Jørn Heggseth Statnett. Alle feil, 1-22 kv 2009-2013. Spreadsheet received 19th of January 2016 with the complete list of faults registered in the Norwegian power grid, 1-22 kV 2009-2013. The complete spreadsheet is excepted from public disclosure.

[18] Helge Seljeseth Statnett. Examples of voltage dips measured in the norwegian distribution grid.

[19] Tina D. Bystøl. Stabilitetsproblemer i distribusjonsnett med lokal kraftproduksjon, 2007.

[20] Gravbrotfoss. `http://www.fadumtekniske.no/WEB%20GRAVBROTFOSS/18012009%20REFERANSESIDE%20GRAVBROTFOSS.htm`. Accessed: 2016-05-10.

[21] Vannkraft i nord-trønderlag. `https://no.wikipedia.org/wiki/Kategori:Vannkraftverk_i_Nord-Tr%C3%B8ndelag`. Accessed: 2016-05-10.

[22] Rune Paulsen NTE. Email forwarded from Henrik Kirkeby, SINTEF Energi to Kristine Mamen Antonsen, 06.10.2015 09:50.

[23] SINTEF Energi Arne Petter Brede. *Notat - Montering og drift av 8 MVA, 10-30 kV, mobilt koplingsanlegg DIP LAB*, 2015.

[24] Smaakraft.no. `http://www.smaakraft.no/aktuelt/nyhetsarkiv/bruvollelva-kraftverk_-snasa`. Accessed: 2016-05-10.

[25] Copper impedance. `http://www.electricalengineeringtoolbox.com/2016/01/resistance-and-reactance-per-km-of.html`. Accessed: 2016-04-25.

[26] ENTSO-E. *IMPLEMENTATION GUIDELINE FOR NETWORK CODE "Requirements for Grid Connection Applicable to all Generators"*, 2013.

[27] Småkraft. *Dokumentasjon av høyspenningsanlegget på Bruvollelva*, 2009.

[28] P. C. Sen. *Principles of Electric Machines and Power Electronics*. John Wiley and Sons, 1996.

[29] K. Bonfert. *Betriebsverhalten der synchronmaschine*. Springer Werlag, 1962.

[30] Metal densities. `http://www.engineeringtoolbox.com/metal-alloys-densities-d_50.html`. Accessed: 2016-04-25.

Appendices

A | Simulation Parameters, Snåsa

A.1 Short Circuit Capacity

Resultat fra kortslutningsberegninger i 61195 Bruvollelva.
Knutepunktet er ett 22.000 kV IT-nett.
Nærmeste transformator :
Primærside : SNÅSA-66T1 Merkespenning : 65.000 kV
Sekundærside : SNÅSA-22AY1 Merkespenning : 22.000 kV
Koplingsgruppe : YNyn0 Merkeytelse : 15000 kVA
Max. kortslutningsstrømmer : Temp (C) Faktor
3-polt kortslutning : 3.503 kA
2-polt kortslutning : 3.034 kA 20.0 1.10
Kortslutningsytelse : 133.484 MVA
Imp. pluss-systemet R: 0.452 Ohm X: 3.963 Ohm Z: 3.988 Ohm Cos(phi): 0.113
Min. kortslutningsstrømmer : Temp (C) Faktor
3-polt kortslutning : 3.273 kA
2-polt kortslutning : 2.834 kA 90.0 1.00
Kortslutningsytelse : 124.715 MVA
Imp. pluss-systemet R: 0.476 Ohm X: 3.852 Ohm Z: 3.881 Ohm Cos(phi): 0.123

Figure A.1: *Forwarded email from NTE regarding the short circuit capacity at Bruvollelva power plant*
Source: *[22]*

A.2 Data Sheets for Bruvollelva Power Plant

Bruvollelva Power Plant

Rotor med utpregete poler/Rotor with distinct poles
Sylindrisk rotor /Cylindrical rotor
Cylindrical rotor

Nr.	Data	Symbol	Unit	Value	Appendix
1	Brand	-	-	Končar Generators and Motors Inc.	
2	Type	-	-	6SBV6 710M1-8	
3	Model (year)	-	-	2009	
4	Rated Power	S_N	[MVA]	4,335	
5	Rated voltage	U_N	[kV]	6,6	
6	Rated frequency	F_N	[Hz]	50	
7	Rated power factor	$\cos\ddot{o}_N$	-	0,9	
8	Number of poles (2 times the number of pole pairs)	n_p	-	8	
9	Rotating synchronous speed	n_0	[rpm]	750	
10	Inertia constant	H	[s]	0,370	
11	Moment of inertia	J	[kgm^2]	520	
12	Direct axis synchronous reactance	X_d	[pu]	2,36	
13	Direct axis transient reactance	X'_d	[pu]	0,249	
14	Direct axis subtransient reactance	X''_d	[pu]	0,161	
15	Quadrature axis synchronous reactance	X_q	[pu]	2,32	
16	Quadrature axis transient reactance	X'_q	[pu]	2,32	
17	Quadrature axis subtransient reactance	X''_q	[pu]	0,189	
18	Armature time constant	T_a	[s]	0,067	
19	Armature resistance	r_a	[pu]	0,0068	at 20°C
20	Leakage reactance	X_l	[pu]	0,151	
21	Direct axis open-circuit transient time constant	T_{d0}'	[s]	1,750	
22	Direct axis open-circuit subtransient time constant	T_{d0}''	[s]	0,092	
23	Quadrature axis open-circuit transient time constant	T_{q0}'	[s]	-	
24	Quadrature axis open-circuit subtransient time constant	T_{q0}''	[s]	0,090	
25	Direct axis short-circuit transient time constant	T_d'	[s]	0,184	
26	Direct axis short-circuit subtransient time constant	T_d''	[s]	0,059	
27	Quadrature axis short-circuit transient time constant	T_q'	[s]	-	
28	Quadrature axis short-circuit subtransient time constant	T_q''	[s]	0,007	
29	Zero sequence resistance	R_0	[pu]	0,0069	at 20°C
30	Zero sequence reactance	X_0	[pu]	0,092	

Figure A.2: *Data sheet for Bruvollelva power plant page 1*
Source: *Småkraft*

31	Neutral earthing resistor	R_e	[Ù]	Not in scope of supply

CT Protection **-Strømtransformatorer, vern**

Tabell 9

Nr.	CT - Data strømtransformator		Enhet	Verdi	Vedlegg
1	Typebetegnelse	Type	-	INA2-12	
2	Fabrikat		-	Končar Instrument transformers Inc.	
3	Måleklasse	Class	-	5P10 / 5P10	
4	Anvendt omsetningsforhold	Ratio	[A/A]	500/1/1	
5	Byrde	Burden	[VA]	10 / 10	
6	Ytelse		[VA]		

VT -Spenningstransformatorer

Tabell 7

Nr.	VT- Data spenningstransformator		Enhet	Verdi	Vedlegg
1	Typebetegnelse	Type	-	4VPA1-12	
2	Fabrikat		-	Končar Instrument transformers Inc.	
3	Måleklasse	Class	-	1,0	
4	Anvendt omsetningsforhold	Ratio	[V/V]	3810,5/110	
5	Byrde Burden		[VA]	5	
6	Ytelse		[VA]		
7	Beregnet spenningsfall i leder		[%]	0,053	
8	Byrdeberegning		-	-	
9	Kopi av prøveprotokoll		-	attached	

Figure A.3: *Data sheet for Bruvollelva power plant page 2*
Source: *Småkraft*

A.3 Protection Relays at Bruvollelva Power Plant

Table A.1: *Generator protection relays at Bruvollelva power plant*
Source: *[27]*

Relay description	Values of function	Release time	Function
Reverse power relay (ANSI 32)	-P $\leq$ -5% Pn	2 s	Stop
Over current (ANSI 50/51)	116 % In	1.5 s	Disconnection
Over current (ANSI 50/51)	350 % In	0.5 s	Stop
Gen. over voltage (ANSI 59)	107 % Un	1.4 s	Stop
Gen. over voltage (ANSI 59)	115 % Un	0.1 s	Stop
Gen. under voltage (ANSI 27)	90 % Un	1.4 s	Disconnection
Gen. under voltage (ANSI 27)	80 % Un	0.1 s	Disconnection
Bus over voltage (ANSI 59)	107 % Un	1.4 s	Stop
Bus over voltage (ANSI 59)	115 % Un	0.1 s	Stop
Bus under voltage (ANSI 27)	92 % Un	5 s	Disconnection
Bus under voltage (ANSI 27)	80 % Un	0.1 s	Disconnection
Gen. over frequency (ANSI 81O)	51 Hz	0.2 s	Stop
Gen. under frequency (ANSI 81U)	49 Hz	0.2 s	Stop
Bus over frequency (ANSI 81O)	51 Hz	0.1 s	Stop
Bus under frequency (ANSI 81U)	49 Hz	0.2 s	Stop
Bus under frequency (ANSI 81U)	48 Hz	0.1 s	Stop
Gen. over load (ANSI 32)	P $\geq$ 120 %Pn	10 s	Alarm
Unbalanced current (ANSI 46)	Unb. osc. = 8 % In	10 s	Stop
Unbalanced voltage (ANSI 47)	Unb. osc. = 20 % Un	12 s	Stop
Reactive power import (ANSI 32)	42.2 % Pn	1.5 s	Stop
Reactive power export (ANSI 32)	66.7 % Pn	1.5 s	Stop
Out of step relay (ANSI 78)	Voltage angle step 20 °		Stop

Table A.2: *Over current relays placed at the 22 kV side of the transformer at Bruvollelva power plant*
Source: *[27]*

Relay description	Values of function	Release time	Function
Over current	125 % In	1.5 s	Disconnection
Over current	397 %	0.05 s	Disconnection
Earth fault	Uo $\leq$ 22.73 %Uo,n	3 s	Stop

B | Parameter Calculations for the lab machine

B.1 Stator Resistance

Figure B.1 shows an equivalent circuit of a synchronous generator. E_f is the field voltage, X_{ar} and X_{al} the synchronous reactance, and R_a represents the effective resistance in the circuit. This resistance includes effects such as operating temperature and skin effects, and may be measured by use of an milliohm-meter.

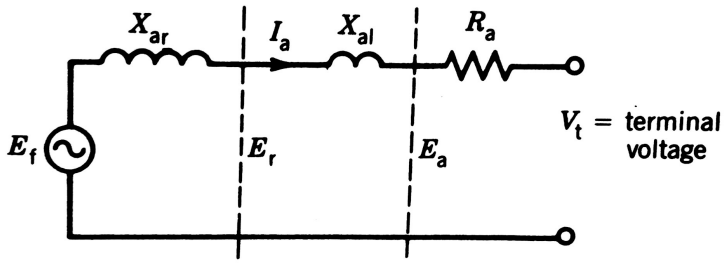

Figure B.1: *Equivalent circuit of the synchronous generator*
Source: *[28]*

The milliohm-meter measured the resistance per phase by sending out a small DC current. The voltage was measured, and the resistance calculated. The test was made when the machine was turned off, and the measurements were made on all three phases to verify the result.

$$X_{base} = \frac{(400V)^2}{1000VA} = 160\Omega \tag{B.1}$$

$$R_a = 10.6\Omega = \frac{10.6\Omega}{X_{base}} p.u. = 0.066 p.u. \tag{B.2}$$

B.2 Transient Reactances and Time Constants

When studying a synchronous generator under transient conditions, the transient reactances and time constants are important parameters for understanding the behaviour. To calculate these values, a short circuit test was accomplished.

B.2.1 Test Method

The setup can be seen in figure B.2 The generator terminals were connected to a relay,

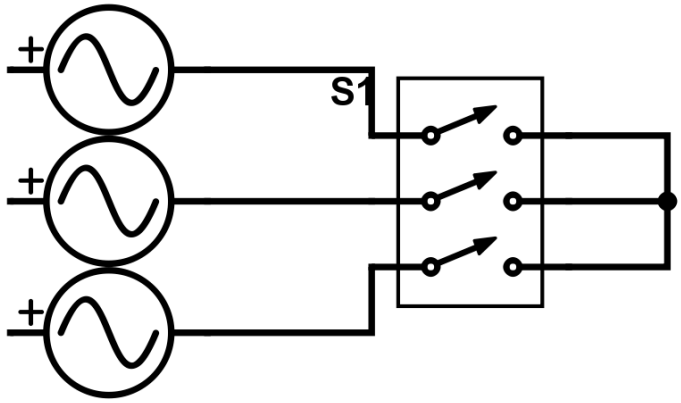

Figure B.2: *Short circuit test setup*

controlled by a manual switch. The other side of the relay was short circuited. For the experiment, the synchronous motor was first used as the prime mover, but the protection system made the test impossible. An AC machine was therefore used instead.

A transistor controlled electronic relay was used for the first tests. The relay had a delay measured to be approximately 5 ms from the start to the end of the swiching process, resulting in in a short circuit current where the first peak were missing. The relay was therefore changed to a mechanical relay. This gave a faster reaction, but some oscillations appeared in the plots due to the the mechanical collision during closing.

During the test, the short circuit current was plotted. When a three phase fault occur, several components of current will flow in the generator. Each phase can be represented as the sum of a DC current and a symmetrical AC component. This is because the generator is inductive before the fault, and a current in an inductor cannot change instantly. The AC component will rise immediately when the fault happens, and because the total current will have to be constant just after the fault, a DC component arises.

It is the AC symmetrical current that is relevant for calculating the transient reactances, and the current did therefore have to be cut at a zero passage. This makes the DC component zero, making it easier to study the AC component. An oscilloscope was used

to plot one of the phases, and the results from each test was saved to a csv file. The test was made 25 times, to make good chances of a good plot.

The short circuit current may be divided into three different parts, as seen in equation B.3. That is a subtransient part, only lasting for a few milliseconds, a transient period lasting a little longer, and a steady state period.

$$I_{sc} = I_{ss} + (I' - I_{ss})e^{-t/T'_d} + (I'' - I')e^{-t/T''_d} \tag{B.3}$$

The three different periods are easy to see when plotting the magnitude of the current in a semi-logaritmic plot, as the slope change fast. An example of the AC-component of a short circuit current and a semi-logaritmic plot of the current magnitude is shown in figure B.3 and B.4.

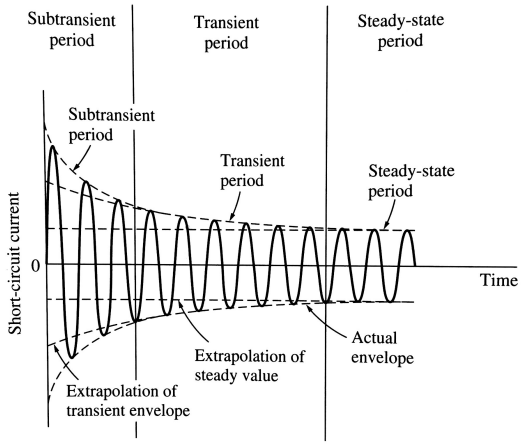

Figure B.3: *Symmetrical short circuit current*
Source: *[12]*

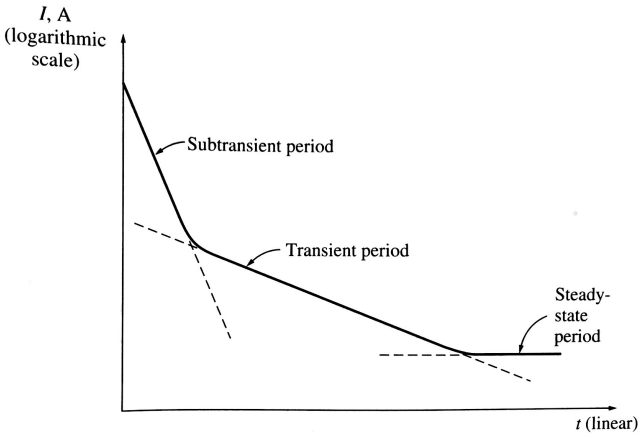

Figure B.4: *Semi logarithmic plot of the current magnitude*
Source: *[12]*

The values of I_{ss}, I', I'', T'_d and T''_d can be calculated from the plot. Finally, the three direct axis reactances can be calculated by use of equation B.4-B.6

$$X_d = \frac{E_A}{I_{ss}} \tag{B.4}$$

$$X'_d = \frac{E_A}{I'} \tag{B.5}$$

$$X''_d = \frac{E_A}{I''} \tag{B.6}$$

B.3 Test Results and Calculations

A plot of the measured short circuit current is given in figure B.5.

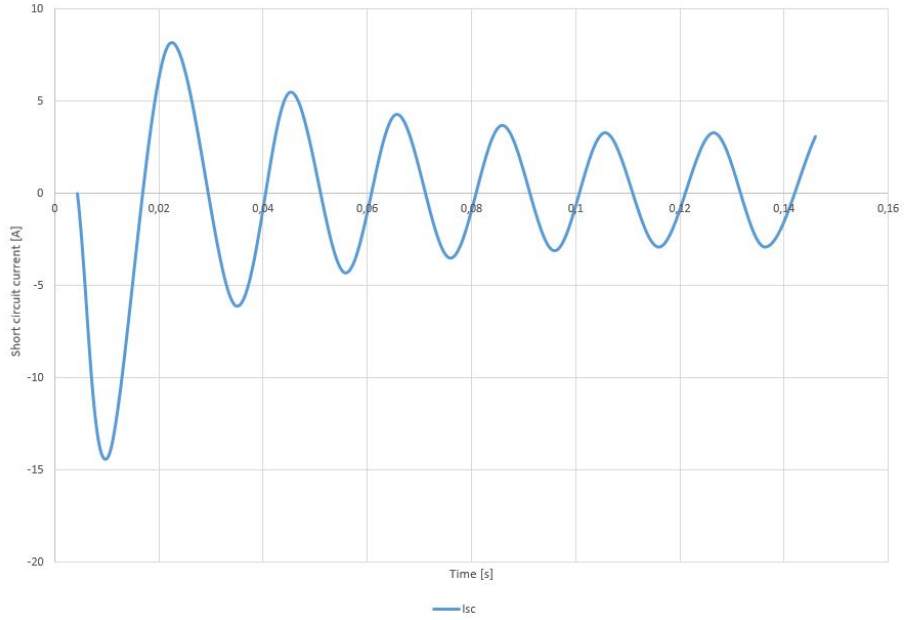

Figure B.5: *Measured short circuit current in phase a*

As seen in figure B.3, the steady state current is the current after the transient period, where the amplitude is stable.

$$I_{ss} = 3,2A \tag{B.7}$$

A semilogarithmic plot is seen in figure B.6.

Since the subtransient time constant is assumed to be significantly smaller than the transient time constant, the contribution from the subtransient part of the current can be negilected in the last part of the plot. Equation (B.3) can therefore be rewritten for t larger than one period.

$$I - I_{ss} \approx (I' - I_{ss})e^{-t/T'_d} \tag{B.8}$$

By taking the logarithm on both sides, the equation becomes linear. By linear regression, lines describing each period are made. The lines can be seen in figure B.6. The values I' and T' can then be calculated using equation (B.9)

$$ln(I' - I_{ss}) - \frac{t}{T'_d} = 1,66 - 25.64t \tag{B.9}$$

$$I' = e^{1,66} + I_{ss} = 5,26 + 3,2 = 8,46A \tag{B.10}$$

$$T'_d = \frac{1}{25.64} = 0,039s \tag{B.11}$$

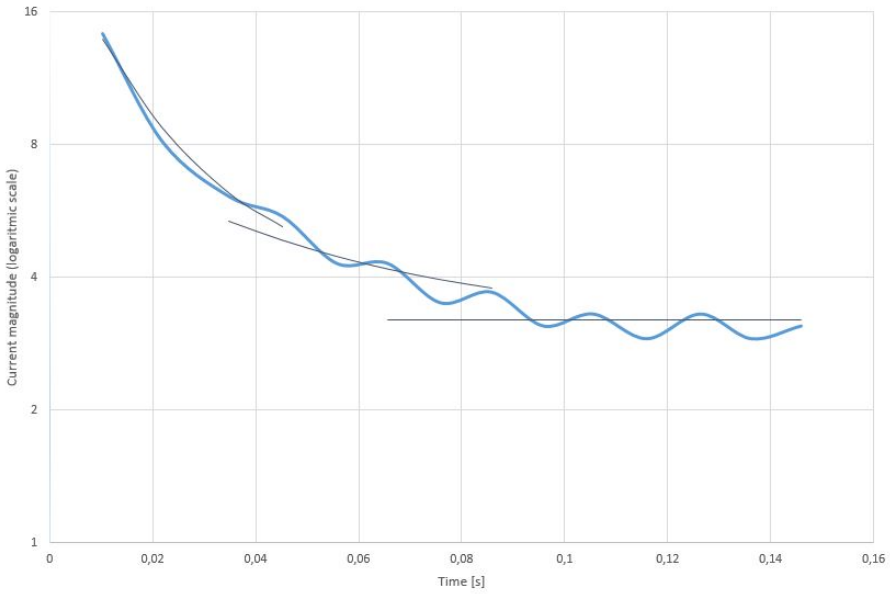

Figure B.6: *The short circuit current in a semi logarithmic plot. Linear functions describing each of the periods are added to the figure.*

The third component of the current can be found by subtracting the two other components from the peak values of the short circuit current. The peaks of the current can then be plotted in a logarithmic plot, and the magnitude of I" and time constant can be found by regression, using the same method as for the transient components.

$$ln(I'' - I') - \frac{t}{T_d''} = 2,75 - 83,00t \tag{B.12}$$

$$I'' = e^{2,75} + I'' = 15,49 + 8,46 = 24,10A \tag{B.13}$$

$$T_d'' = \frac{1}{83,00} = 0,012s \tag{B.14}$$

Finally, the direct axis reactances can be calculated:

$$X_d = \frac{E_A}{I_{ss}} = \frac{400V}{3,2A} = 125\Omega = \frac{125\Omega}{X_{base}}p.u. = 0,78p.u \tag{B.15}$$

$$X_d' = \frac{400V}{8,46A} = 47,28\Omega = 0,29p.u. \tag{B.16}$$

$$X_d'' = \frac{400V}{24,10} = 16,60\Omega = 0,10p.u. \tag{B.17}$$

There are many sources off error in these calculations, as there is a large span of values that give a tolerable linear regression. The extrapolation envelopes for each period given from the calculated values are therefore plotted in figure B.7 to verify the results. The

values seem to be realistic.

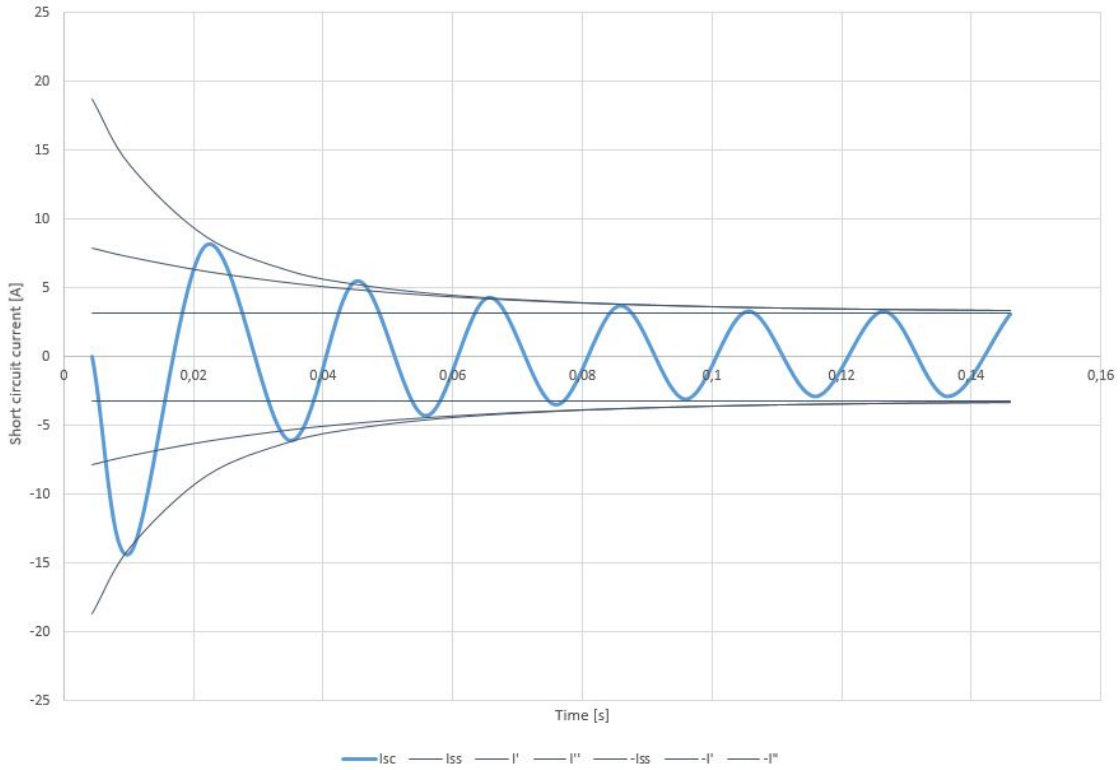

Figure B.7: *Short circuit current in one phase with lines showing the steady state, transient and subtransient envelope*

To simulate the generator in the simulation program SIMPOW, the parameters T'_{d0}, T''_{d0}, T'_{q0} and T'_{q0} were required. The direct axis open-circuit time constants are calculated by equation (B.18) and (B.19). X_N is here the system reactance. For simplicity, this is assumed to be zero.

$$T'_{d0} = \frac{X_d + X_N}{X'_d + X_N} \cdot T'_d \approx \frac{X_d}{X'_d} \cdot T'_d = \frac{0.78}{0.30} \cdot 0.039s = 0.10s \tag{B.18}$$

$$T''_{d0} = \frac{X'_d + X_N}{X''_d + X_N} \cdot T''_d \approx \frac{X'_d}{X''_d} \cdot T''_d = \frac{0.3}{0.10} \cdot 0.012s = 0.036s \tag{B.19}$$

The direct axis is centred on the north pole, and the quadrature axis is placed 90° electrically ahead. The quadrature axis time constants are assumed to be equal to the direct axis time constants. The quadrature axis reactances are calculated due to the assumption that the machine has salient poles and damper windings. For salient poles, X_q equals $0.65X_d$, and X'_q equals X_q. For a "complete" damper winding, the direct axis and quadrature axis subtransient reactances are equal[29].

$$X_q = 0.65 \cdot X_d = 0.65 \cdot 0.78 p.u. = 0.507 p.u. \tag{B.20}$$
$$X'_q = X_q = 0.507 p.u. \tag{B.21}$$
$$X''_q = X''_d = 0.10 p.u. \tag{B.22}$$

The parameter XA in SIMPOW refers to the stator leakage reactance, marked as X_{al} in figure B.1. This is usually about 10 % of the direct axis reactance[9].

$$X_A = 0.10 \cdot X_d = 0.08 p.u. \tag{B.23}$$

B.4 Saturation

The saturation curve is not given for the machine, so in the generator model, the parameters SE1 and SE2 had to be guessed. A typical saturation curve is given in figure B.8. The linear line shows the open circuit characteristic describes the behaviour of a saturated machine.

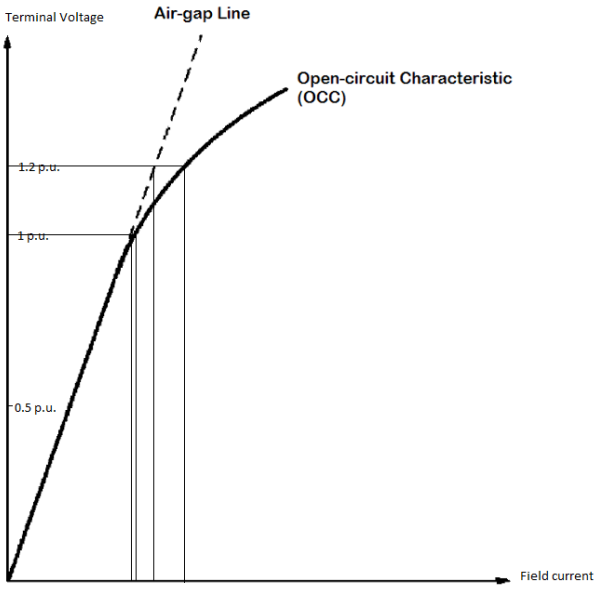

Figure B.8: *Saturation curve for a synchronous generator*

The parameter SE1 is comparing the field current in the generator at rated terminal voltage (1 p.u.) with the unsaturated line. SE2 describes the same error at 1.2 times rated voltage. Since there is no data sheet given for the machine, and no open circuit test is made, the values are guessed for simulation purpose. The lab machine is assumed to be well dimensioned.

$$SE1 = 0.05 \tag{B.24}$$
$$SE2 = 0.1 \tag{B.25}$$

B.5 Inertia Constant

The inertia constant is defined as the kinetic energy in the rotor at rated values, divided to the rated power.

$$H = \frac{E_k}{S_n} = \frac{\frac{1}{2}J\omega^2}{S_n} \tag{B.26}$$

By assuming the rotor to be a solid cylinder, the moment of inertia can be calculated by using equation (B.27).

$$J = \frac{1}{2}mr^2 \tag{B.27}$$

The mass is the mass density integrated over the volume of the cylinder. Inserting equation (B.27) into (B.26), the H-constant can be expressed

$$H = \frac{\frac{1}{4}mr^2\omega^2}{S_n} \tag{B.28}$$

The length and radius of the rotor were measured approximately, as the shield made it difficult to make precise measurements. The results are presented in table B.1. The material were assumed to be steel, which has a mass density of 7850 kg/m^3 [30].

Table B.1: *Rotor measurements*

Parameter	Length
Diameter	9 cm
Length	15 cm

The values are inserted in equation (B.28), and the inertia constant are calculated in (B.32)

$$H = \frac{\frac{1}{4}mr^2\omega^2}{S_n} \tag{B.29}$$

$$H = \frac{\frac{1}{4}\cdot\rho\cdot\pi\cdot r^2\cdot l\cdot r^2\cdot\omega^2}{S_n} \tag{B.30}$$

$$H = \frac{\frac{1}{4}\cdot 7850kg/m^3\cdot\pi\cdot(0.045m)^2\cdot(0.15m)\cdot(0.045m)^2\cdot(1500\frac{rounds}{min}\cdot\frac{2\pi}{60s})^2}{1kW} \tag{B.31}$$

$$H = 0.094s \tag{B.32}$$

C | List of equipment, In-house lab

The right column describes for which experiment the equipment was used. "S.C" stands for the short circuit test used to calculate the parameters of the machine. "DIP" stands for the actual dip tests, and "both" means that the equipment was used for both the short circuit and the dip-tests.

Number	Description	Type	NTNU ID	Used for
1	Mechanical Relay	Moeller DIL M17-10	-	S.C.
2	Ansynch. prime mover	LEYBOLD 1kW	A03-0092	S.C.
3	Synch. generator	LEYBOLD 73306 class 1,0	A02-0034	both
4	Oscilloscope	Tektronix MSO 2014	G04-0344	both
5	Synchronization Relay	LEYBOLD manual synch. unit	R04-0175	both
6	Motor protector switch	LEYBOLD	R04-0182	both
7	Excitation voltage controller	LEYBOLD	B02-0691	both
8	Frequency converter	LEYBOLD	B03-0503	both
9	Current probe	Fluke 80i - 110s	I04-0488	both
10	Differential probe	GE8115	I06-0430	both
11	Power switch	manual elco switch	-	S.C.
12	Power quality data analyser	ELSPEC G4420	SINTEF H02-0187	both
13	Solid state relay	GNA5 8413910	-	dip
14	Signal generator	Tektronix AFG3052C Dual channel	B03-0494	dip
15	3 ph inductance	NTNU produced, 47mH	K02-0013	dip
16	3 ph inductance	NTNU produced, 47mH	K02-0014	dip
17	3 ph cable	PR $3 \cdot 1.5mm^2$	-	dip
18	Milliohm meter	Instek GOM-802	H01-0096	dip

D | SIMPOW files

D.1 Realistic Case

```
realistisk_optpow

Snaasa
**
GENERAL
  SN=25    !snåsa transformer rating
END

NODES
  BUS1  UB=66   AREA=1
  BUS2  UB=66   AREA=1
  BUS3  UB=22   AREA=2
  BUS33 UB=22   AREA=2
  BUS4  UB=22   AREA=2
  BUS5  UB=22   AREA=2
  BUS6  UB=22   AREA=2
  BUS7  UB=22   AREA=2
  BUS8  UB=22   AREA=2
  BUS9  UB=22   AREA=2
  BUS10 UB=22   AREA=2
  BUS11 UB=22   AREA=2
  BUS12 UB=22   AREA=2
  BUS13 UB=22   AREA=2
  BUS14 UB=22   AREA=2
  BUS15 UB=22   AREA=2
  GEN1  UB=6.6  AREA=2   !Gemsa Electrics 4.6MVA
  DIPLAB UB=22  AREA=2   !Her skal diplaben plasseres
  GEN11 UB=6.6  AREA=2   !measuring point
  GEN2  UB=0.69 AREA=2   !Asynkrongenerator
  GEN3  UB=6.6  AREA=2   !Gemsa Electrics 4.6MVA
  GEN33 UB=6.6  AREA=2   !measuring point
  GEN4  UB=0.69 AREA=2   !Alconca 1.6MVA
  GEN44 UB=0.69 AREA=2   !measuring point
END

LINES                                  !Data fra NTE
  BUS1  BUS2  TYPE=1 R=0.1271 X=0.3259 L=0.842    !short line- measuring point for KOMP1
  BUS3  BUS33 TYPE=1 R=0.1    X=0.2    L=0.002

                                       Page 1
```

Figure D.1: *OPTPOW file for realistic case, page 1*

```
                                realistisk_optpow
  BUS3  BUS4  TYPE=1 R=0.151  X=0.344 L=0.38 I1MAX=0.624 !Line1, FeAl 120
  BUS4  BUS5  TYPE=1 R=0.151  X=0.344 L=5.74 I1MAX=0.624 NCON=0 !Line2, FeAl 120
  BUS5  BUS6  TYPE=1 R=0.320  X=0.120 L=0.42 I1MAX=0.275 !Cable3, TXPS KABEL,bruker data for TSLE kabel
  BUS6  BUS7  TYPE=1 R=0.359  X=0.373 L=0.78 I1MAX=0.362 !Line4, FeAl50
  BUS7  BUS8  TYPE=1 R=0.721  X=0.395 L=1.54 I1MAX=0.235 !Line5, FeAl25
  BUS8  BUS14 TYPE=1 R=0.721  X=0.395 L=4.29 I1MAX=0.235 !Line6, FeAl25
  BUS14 BUS15 TYPE=1 R=0.721  X=0.395 L=3.82 I1MAX=0.235 !Line7, FeAl25
  BUS8  BUS9  TYPE=1 R=0.721  X=0.395 L=5.67 I1MAX=0.235 !Line8, FeAl25
  BUS9  BUS11 TYPE=1 R=0.721  X=0.395 L=0.24 I1MAX=0.235 !Line9, FeAl25
  BUS11 BUS12 TYPE=1 R=0.320  X=0.120 L=0.14 I1MAX=0.275 !Cable10, TSLE KABEL
  BUS12 BUS13 TYPE=1 R=1.721  X=0.395 L=1.58 I1MAX=0.235 !Line11, FeAl25
  BUS9  BUS10 TYPE=1 R=0.721  X=0.395 L=4.79 I1MAX=0.235 !Line12, FeAl25
  BUS4  DIPLAB TYPE 0                                     !Short circuit in parallel to Xsr
  GEN1  GEN11 TYPE=1 R=0.1    X=0.200 L=0.002             !short line- measuring point for AVR
  GEN3  GEN33 TYPE=1 R=0.1    X=0.200 L=0.002             !short line- measuring point for AVR
  GEN4  GEN44 TYPE=1 R=0.1    X=0.200 L=0.002             !short line- measuring point for AVR
END

TRANSFORMERS
  BUS2 BUS33  SN=25  UN1=66    UN2=22 NW=2 EX12=0.07523 ER12=0.00320 !Power transformer snåsa, R. Paulsen mail
9.08.07
                                    TAPSIDE=2                        !Tapside is the 22kV side
                                    STEP=1.105 +NSTEP=4 -NSTEP=4     !Tap step size and nr of steps, NTE
  GEN11 DIPLAB  SN=6   UN1=6.6  UN2=22 NW=2 ER12=0.006   EX12=0.06     !DG1,Toftevaag 4MVA, 6.6/22kV er12=0.006
ex12=0.06
  GEN2  BUS14 SN=1   UN1=0.69 UN2=22 NW=2 ER12=0.00730 EX12=0.05441  !DG2,R.Paulsen mail 9.08.07, 22/0.69kV:
SN=1MVA
  GEN33 BUS15 SN=4   UN1=6.6  UN2=22 NW=2 ER12=0.006   EX12=0.06     !DG3,
  GEN44 BUS13 SN=4   UN1=0.69 UN2=22 NW=2 ER12=0.00720 EX12=0.0583   !DG4,Toftevaag 1.6MVA,0.69/22kV er12=0.0072
ex12=0.0583
END

LOADS
   BUS3  P=2.71 Q=0.71 MP=1
   BUS5  P=1.05 Q=0.25 MP=1
   BUS6  P=1.00 Q=0.10 MP=1

                                                                Page 2
```

Figure D.2: *OPTPOW file for realistic case, page 2*

```
realistisk_optpow

  BUS7  P=0.55 Q=0.09 MP=1
  BUS8  P=0.55 Q=0.09 MP=1
  BUS9  P=0.55 Q=0.09 MP=1
  BUS10 P=0.55 Q=0.09 MP=1
END

SHUNT IMPEDANCES
  GEN2 UN=0.69 Q=-0.58 NCON=0
  BUS3 UN=22   Q=-1.96 NCON=0
END

TABLES
1 TYPE=2 F= -1  0.02    !Re (rotor resistance) as a function of the slip! constant, Re=0.02
            1  0.02
END

BREAKERS
  1 TYPE=0
END

POWER CONTROL
  BUS1 TYPE=NODE NAME=STIFF RTYP=SW  U=66   FI=0

  GEN1 TYPE=NODE NAME=DG1   !RTYP=UP  U=6.6  P=4.2 !case 3
                            RTYP=PQ   P=3.9  Q=0 !case 4        Q=0.
  GEN4 TYPE=NODE NAME=DG4   !RTYP=UP  U=0.69 P=2.1 !case 3
                            RTYP=PQ   P=2.1  Q=1. NCON=0 !case 4      Q=0.
END
END
```


Figure D.3: *OPTPOW file for realistic case, page 3*

```
realistisk

Snaasa
**
CONTROL DATA
 TEND=10 !stop simulation (time)  TEND=10   20  150
 SPL=0.05
 TETL=180
! DEND=-1 skips presimulation
END

GENERAL
 FN=50    !frequnecy
 REF=BUS1 !infinite bus is used as referance machine
END

FAULTS
 F1 TYPE=3PSG NODE GEN11 R=0
END

RUN INSTRUCTION
AT 1.000 INST CONNECT FAULT F1
AT 1.075 INST DISCONNECT FAULT F1
END

NODES
 BUS1 TYPE=1 R=2 X=20
END

SYNCHRONOUS MACHINE
!3 ph generator, salient poles for hydro applications, Bruvollelva kraftverk:SV 100/70/6
DG1 GEN1 TYPE=2                                    !TYPE2: one field winding,one damper winding in
d-axis,
                                                    !one damper winding in q-axis. Saturation excluded
        SN=4.33 UN=6.6                              !Inertia constant and damping constant
        H=0.370 D=0 !H=2                           !Reactances[p.u] d- axis
        XD=2.36 XDP=0.249 XDB=0.1675               !Reactances[p.u] q- axis
        XQ=2.32 XQB=0.189                           !open circuit subtransient and transient time
        TDOP=1.750 TDOB=0.092 TQOB=0.090

                                                    Page 1
```

Figure D.4: *DYNPOW file for realistic case, page 1*

```
                                        realistisk
constants
!               X0=0.092 X2=0.2827                          !Zero sequence reactance and negative sequence
reactance
                XA=0.151 RA=0.0068                          !Armature reactance and resistance
                V1D=1.0 V2D=1.2 SE1D=0.1 SE2D=0.3          !Saturation
                VREG=10                                     !Voltage regulator identification number  VREG=6
                TURB=0                                      !  TURB=101


!!3 ph generator with cylindrical rotor, Alconza-Berango, S.L Type NIIR5060 A-4LW
DG4 GEN4  TYPE=3                                            !TYPE3: Model with one field winding and no damper
windings.
                SN=2.5 UN=0.69                              !one damper winding in q-axis. Saturation excluded
                H=1 D=0 !H=2                                !Inertia constant and damping constant
                XD=2.656 XDP=0.136 XDB=0.098                !Reactances[p.u] d- axis
                XQ=2.527 XQB=0.105                          !Reactances[p.u] q- axis
                TDOP=3.3997                                 !open circuit transient time constants
                X0=0.125 X2=0.348                           !Zero sequence reactance and negative sequence
reactance
                XA=0.1 RA=0.00219                           !Armature reactance and resistance
                V1D=1.0 V2D=1.2 SE1D=0.1 SE2D=0.3          !Saturation
                VREG=2    !5  or 8                                    !Voltage regulator identification number
END

REGULATORS
!for DG1 and DG3
1 TYPE=DSL/EXCITERAC8B/ E1=2.222 SE1=1.346 E2=2.962 SE2=1.9
                         TE=0.5 KE=1.0 TA=0 VRMIN=0 VRMAX=35 KA=1.0
                         TD=0.01 KD=24 KI=145 KP=150
!for DG4
 2 TYPE=DSL/EXCITERAC8B/ E1=2.222 SE1=1.346 E2=2.962 SE2=1.9
                        TE=0.5 KE=1.0 TA=0 VRMIN=0 VRMAX=10 KA=1.0
                        TD=0.01 KD=25 KI=150 KP=160

!Bruvollelva, values from the AVR at Snaasa, Var mode
9 TYPE=DSL/EXCITERSIN/  E1=2.222 SE1=1.346 E2=2.962 SE2=1.9
                                          Page 2
```

Figure D.5: *DYNPOW file for realistic case, page 2*

```
                                                realistisk
                          YMIN=-0.1 YMAX=0.1 VMAX=0.1 KII=3.0 VMIN=-0.1  KG=1.0
                          TE=0.5 KE=1.0 TA=0 VRMIN=0 VRMAX=10 KA=1.0
                          TD=0.08 KD=66.3 KI=148.5 KP=177.2
                          NREG=GEN1 GEN11

!Bruvollelva, values from the AVR at Snaasa, PF mode
10 TYPE=DSL/EXCITERQE/  E1=2.222 SE1=1.346 E2=2.962 SE2=1.9
                          YMIN=-1 YMAX=1 VMAX=1 KII=10 VMIN=-1 KG=1
                          TE=0.5 KE=1.0 TA=0 VRMIN=-1 VRMAX=10 KA=1.0
                          TD=0.08 KD=66.3 KI=148.5 KP=177.2
                          NREG=GEN1 GEN11
END

DSL-TYPES
!Automatic voltage regulator (AVR)
 EXCITERAC8B(E1,SE1,E2,SE2,VC,TI/1/,TE,KE,TA,VRMIN,VRMAX,KA,TD,KD,KI,KP,UF,UF0)

 !AVR with VAR control (reactive power)
 EXCITERQE(E1,SE1,E2,SE2,VC,QE,YMIN,YMAX,VMAX,KII,TII/1/,VMIN,KG,TI/1/,TE,KE,TA,
           VRMIN,VRMAX,KA,TD,KD,KI,KP,UF,UF0)

 !AVR with sinfi control (power factor control)
 EXCITERSIN(E1,SE1,E2,SE2,VC,PE,QE,YMIN,YMAX,VMAX,KII,TII/1/,VMIN,KG,TI/1/,TE,KE,TA,
            VRMIN,VRMAX,KA,TD,KD,KI,KP,UF,UF0)
END

TURBINES
 101   TYPE 22 TAB 10
END

BREAKERS
 1 TYPE=0
END

END

                                                Page 3
```

Figure D.6: *DYNPOW file for realistic case, page 3*

D.2 Realistic Case Without Voltage Angle Impact

```
                realsitisk_uten_vinkel_dynpow
Snaasa
**
CONTROL DATA
 TEND=10 !stop simulation (time)  TEND=10   20  150
  SPL=0.05
  TETL=180
 ! DEND=-1 skips presimulation
END

GENERAL
  FN=50     !frequnecy
  REF=BUS1 !infinite bus is used as referance machine
END

TABLE
59  TYPE=0  F
$include table_realistisk_4_gen11_2805.txt
END

NODES
  BUS1 TYPE=1 R=2 X=20
  GEN11 TYPE=4 UTAB=59
END

SYNCHRONOUS MACHINE
!3 ph generator, salient poles for hydro applications, Bruvollelva kraftverk:SV 100/70/6
DG1 GEN1 TYPE=2                          !TYPE2: one field winding,one damper winding in
d-axis,
                SN=4.33 UN=6.6             !one damper winding in q-axis. Saturation excluded
                H=0.370 D=0 !H=2           !Inertia constant and damping constant
                XD=2.36 XDP=0.249 XDB=0.1675  !Reactances[p.u] d- axis
                XQ=2.32 XQB=0.189          !Reactances[p.u] q- axis
                TDOP=1.750 TDOB=0.092 TQOB=0.090   !open circuit subtransient and transient time
constants
!               X0=0.092 X2=0.2827         !Zero sequence reactance and negative sequence
reactance
                                                                    Page 1
```

Figure D.7: *DYNPOW file for realistic case without voltage angle impact, page 1*

```
                realsitisk_uten_vinkel_dynpow
      XA=0.151 RA=0.0068                !Armature reactance and resistance
      V1D=1.0 V2D=1.2 SE1D=0.1 SE2D=0.3 !Saturation
      VREG=10                           !Voltage regulator identification number  VREG=6
      TURB=0                            !  TURB=101

!!3 ph generator with cylindrical rotor, Alconza-Berango, S.L Type NIIR5060 A-4LW
DG4 GEN4  TYPE=3                        !TYPE3: Model with one field winding and no damper
windings.
                SN=2.5 UN=0.69          !one damper winding in q-axis. Saturation excluded
                H=1 D=0 !H=2            !Inertia constant and damping constant
                XD=2.656 XDP=0.136 XDB=0.098  !Reactances[p.u] d- axis
                XQ=2.527 XQB=0.105      !Reactances[p.u] q- axis
                TDOP=3.3997             !open circuit transient time constants
                X0=0.125 X2=0.348       !Zero sequence reactance and negative sequence
        reactance
                XA=0.1 RA=0.00219       !Armature reactance and resistance
                V1D=1.0 V2D=1.2 SE1D=0.1 SE2D=0.3  !Saturation
                VREG=2    !5                !Voltage regulator identification number
        END
        REGULATORS
        !for DG1 and DG3
        1 TYPE=DSL/EXCITERAC8B/ E1=2.222 SE1=1.346 E2=2.962 SE2=1.9
                                TE=0.5 KE=1.0 TA=0 VRMIN=0 VRMAX=35 KA=1.0
                                TD=0.01 KD=24 KI=145 KP=150
        !for DG4
          2 TYPE=DSL/EXCITERAC8B/ E1=2.222 SE1=1.346 E2=2.962 SE2=1.9
                                TE=0.5 KE=1.0 TA=0 VRMIN=0 VRMAX=10 KA=1.0
                                TD=0.01 KD=25 KI=150 KP=160

        !Bruvollelva, values from the AVR at Snaasa, Var mode
        9 TYPE=DSL/EXCITERSIN/  E1=2.222 SE1=1.346 E2=2.962 SE2=1.9
                                YMIN=-0.1 YMAX=0.1 VMAX=0.1 KII=3.0 VMIN=-0.1  KG=1.0
                                TE=0.5 KE=1.0 TA=0 VRMIN=0 VRMAX=10 KA=1.0
                                TD=0.08 KD=66.3 KI=148.5 KP=177.2
                                NREG=GEN1 GEN11
                                                                Page 2
```

Figure D.8: *DYNPOW file for realistic case without voltage angle impact, page 2*

```
realsitisk_uten_vinkel_dynpow

!Bruvollelva, values from the AVR at Snaasa, PF mode
10 TYPE=DSL/EXCITERQE/  E1=2.222 SE1=1.346 E2=2.962 SE2=1.9
                        YMIN=-1 YMAX=1 VMAX=1 KII=10 VMIN=-1 KG=1
                        TE=0.5 KE=1.0 TA=0 VRMIN=-1 VRMAX=10 KA=1.0
                        TD=0.08 KD=66.3 KI=148.5 KP=177.2
                        NREG=GEN1 GEN11
END

DSL-TYPES
!Automatic voltage regulator (AVR)
 EXCITERAC8B(E1,SE1,E2,SE2,VC,TI/1/,TE,KE,TA,VRMIN,VRMAX,KA,TD,KD,KI,KP,UF,UF0)

 !AVR with VAR control (reactive power)
EXCITERQE(E1,SE1,E2,SE2,VC,QE,YMIN,YMAX,VMAX,KII,TII/1/,VMIN,KG,TI/1/,TE,KE,TA,
          VRMIN,VRMAX,KA,TD,KD,KI,KP,UF,UF0)

 !AVR with sinfi control (power factor control)
EXCITERSIN(E1,SE1,E2,SE2,VC,PE,QE,YMIN,YMAX,VMAX,KII,TII/1/,VMIN,KG,TI/1/,TE,KE,TA,
           VRMIN,VRMAX,KA,TD,KD,KI,KP,UF,UF0)
END

TURBINES
 101  TYPE 22 TAB 10
END

BREAKERS
 1 TYPE=0
END
END
```

Page 3

Figure D.9: *DYNPOW file for realistic case without voltage angle impact, page 3*

D.3 DipLab

```
Snaasa,
DIPLAB
**
GENERAL
 SN=25    !snåsa transformer rating
END

SHUNT IMPEDANCES
 GEN2 UN=0.69 Q=-0.58 NCON=0
 BUS3 UN=22   Q=-1.96 NCON=0
 DIPLAB X=144 1BREAKER=1 NCON=1!X.sc
END

SREACTORS
EKSTRA DIPLAB TYPE=1 X=32.95 !Xsr
END

NODES
 BUS1  UB=66    AREA=1
 BUS2  UB=66    AREA=1
 BUS3  UB=22    AREA=2
 BUS33 UB=22    AREA=2
 BUS4  UB=22    AREA=2
 BUS5  UB=22    AREA=2
 BUS6  UB=22    AREA=2
 BUS7  UB=22    AREA=2
 BUS8  UB=22    AREA=2
 BUS9  UB=22    AREA=2
 BUS10 UB=22    AREA=2
 BUS11 UB=22    AREA=2
 BUS12 UB=22    AREA=2
 BUS13 UB=22    AREA=2
 BUS14 UB=22    AREA=2
 BUS15 UB=22    AREA=2
 DIPLAB UB=22  AREA=2  !Her skal diplaben plasseres
 EKSTRA UB=22 AREA=2

                                                    Page 1
```

Figure D.10: *OPTPOW file for DIPLAB case, page 1*

```
                                    DIPLAB

   GEN1  UB=6.6   AREA=2  !Gemsa Electrics 4.6MVA
   GEN11 UB=6.6   AREA=2  !measuring point
   GEN2  UB=0.69  AREA=2  !Asynkrongenerator
   GEN3  UB=6.6   AREA=2  !Gemsa Electrics 4.6MVA
   GEN33 UB=6.6   AREA=2  !measuring point
   GEN4  UB=0.69  AREA=2  !Alconca 1.6MVA
   GEN44 UB=0.69  AREA=2  !measuring point
END
LINES
   BUS1  BUS2  TYPE=1 R=0.1271 X=0.3259 L=0.842          !Data fra NTE
   BUS3  BUS33 TYPE=1 R=0.1    X=0.2    L=0.002          !short line- measuring point for KOMP1
   BUS3  BUS4  TYPE=1 R=0.151  X=0.344 L=0.38 I1MAX=0.624 !Line1, FeAl 120
   BUS4  BUS5  TYPE=1 R=0.151  X=0.344 L=5.74 I1MAX=0.624 NCON=0 !Line2, FeAl 120
   BUS5  BUS6  TYPE=1 R=0.320  X=0.120 L=0.42 I1MAX=0.275 !Cable3, TXPS KABEL,bruker data for TSLE kabel
   BUS6  BUS7  TYPE=1 R=0.359  X=0.373 L=0.78 I1MAX=0.362 !Line4, FeAl50
   BUS7  BUS8  TYPE=1 R=0.721  X=0.395 L=1.54 I1MAX=0.235 !Line5, FeAl25
   BUS8  BUS14 TYPE=1 R=0.721  X=0.395 L=4.29 I1MAX=0.235 !Line6, FeAl25
   BUS14 BUS15 TYPE=1 R=0.721  X=0.395 L=3.82 I1MAX=0.235 !Line7, FeAl25
   BUS8  BUS9  TYPE=1 R=0.721  X=0.395 L=5.67 I1MAX=0.235 !Line8, FeAl25
   BUS9  BUS11 TYPE=1 R=0.721  X=0.395 L=0.24 I1MAX=0.235 !Line9, FeAl25
   BUS11 BUS12 TYPE=1 R=0.320  X=0.120 L=0.14 I1MAX=0.275 !Cable10, TSLE KABEL
   BUS12 BUS13 TYPE=1 R=1.721  X=0.395 L=1.58 I1MAX=0.235 !Line11, FeAl25
   BUS9  BUS10 TYPE=1 R=0.721  X=0.395 L=4.79 I1MAX=0.235 !Line12, FeAl25
   EKSTRA  DIPLAB TYPE=0                                  !Legger inn en kortslutning parallelt med Xsr
   BUS4  EKSTRA TYPE=0
   GEN1  GEN11 TYPE=1 R=0.1    X=0.200 L=0.002            !short line- measuring point for AVR
   GEN3  GEN33 TYPE=1 R=0.1    X=0.200 L=0.002            !short line- measuring point for AVR
   GEN4  GEN44 TYPE=1 R=0.1    X=0.200 L=0.002            !short line- measuring point for AVR
END
TRANSFORMERS
   BUS2 BUS33  SN=25  UN1=66   UN2=22 NW=2 EX12=0.07523 ER12=0.00320 !Power transformer snåsa, R. Paulsen mail
9.08.07
                                   TAPSIDE=2                        !Tapside is the 22kV side
                                   STEP=1.105 +NSTEP=4 -NSTEP=4     !Tap step size and nr of steps, NTE

                                                Page 2
```

Figure D.11: *OPTPOW file for DIPLAB case, page 2*

```
                                DIPLAB
 GEN11 DIPLAB  SN=6   UN1=6.6  UN2=22 NW=2 ER12=0.006   EX12=0.06     !DG1,Toftevaag 4MVA, 6.6/22kV er12=0.006
 ex12=0.06
  GEN2  BUS14 SN=1   UN1=0.69 UN2=22 NW=2 ER12=0.00730 EX12=0.05441  !DG2,R.Paulsen mail 9.08.07, 22/0.69kV:
 SN=1MVA
  GEN33 BUS15 SN=4   UN1=6.6  UN2=22 NW=2 ER12=0.006   EX12=0.06     !DG3,
  GEN44 BUS13 SN=4   UN1=0.69 UN2=22 NW=2 ER12=0.00720 EX12=0.0583   !DG4,Toftevaag 1.6MVA,0.69/22kV er12=0.0072
 ex12=0.0583
 END

 BREAKERS
  1 TYPE=0
 END

 LOADS
    BUS3  P=2.71 Q=0.71 MP=1
    BUS5  P=1.05 Q=0.25 MP=1
    BUS6  P=1.00 Q=0.10 MP=1
    BUS7  P=0.55 Q=0.09 MP=1
    BUS8  P=0.55 Q=0.09 MP=1
    BUS9  P=0.55 Q=0.09 MP=1
    BUS10 P=0.55 Q=0.09 MP=1
 END

 !ASYNCHRONOUS MACHINES
 !DG2 GEN2      TYPE=1A  SN=2.5 UN=0.69          !Type A- stauration excluded, data from toftevaag
 !              H=1.5                            !Inertia constant
 !              R1=0.00619                       !Rotor resistance
 !              X1S=0.135952 C1=0.8 X2S=0.112143 C2=0.7 !Stator and rotor leakage reactance and mag reac. C1 and
 C2, current dependent part p.u (default)
 !              RM=0.088095 XM=3.904762          !Magnetizing resistance and reactance, p.u.
 !              RTAB=1  NCON=0                       !Table of rotor resistance as function of slip. Tab
 nr.1
 !END

 TABLES
 1 TYPE=2 F= -1  0.02    !Re (rotor resistance) as a function of the slip! constant, Re=0.02
                                                                    Page 3
```

Figure D.12: *OPTPOW file for DIPLAB case, page 3*

```
DIPLAB

    1  0.02

END

POWER CONTROL
  BUS1 TYPE=NODE NAME=STIFF RTYP=SW  U=66   FI=0

  GEN1 TYPE=NODE NAME=DG1   !RTYP=UP  U=6.6  P=4.2 !case 3
                            RTYP=PQ   P=3.9  Q=0 !case 4       Q=0.
  ! DG2  TYPE=ASYN RTYP=P     P=0.5
  GEN3 TYPE=NODE NAME=DG3 NCON=1  !RTYP=UP  U=6.6  P=2.6 !case 3
                            RTYP=PQ  P=2.6  Q=1. NCON=1 !case 4       Q=0.

  GEN4 TYPE=NODE NAME=DG4   !RTYP=UP  U=0.69 P=2.1 !case 3
                            RTYP=PQ   P=2.1  Q=0 NCON=0 !case 4       Q=0.

END
END
```

Figure D.13: *OPTPOW file for DIPLAB case, page 4*

```
                                    DIPLAB_dynpow

   Snaasa
   DIPLAB
   **
   CONTROL DATA
     TEND=10 !stop simulation (time)  TEND=10   20  150
     SPL=0.05
     TETL=180
   ! DEND=-1 skips presimulation
   END

   GENERAL
     FN=50     !frequnecy
     REF=BUS1 !infinite bus is used as referance machine
   END

   NODES
     BUS1 TYPE=1 R=2 X=20
   END

   RUN INSTRUCTION
     AT 1.000 INST DISCONNECT LINE EKSTRA DIPLAB
     AT 5.000 INST CONNECT SHUNT DIPLAB
     AT 5.000 INST CLOSE SHUNT DIPLAB 1BREAKER PHASE 123
     AT 5.500 INST OPEN SHUNT DIPLAB 1BREAKER PHASE 123
     AT 6.500 INST CONNECT LINE EKSTRA DIPLAB
   END

   SYNCHRONOUS MACHINE
   !3 ph generator, salient poles for hydro applications, Bruvollelva kraftverk:SV 100/70/6
   DG1 GEN1 TYPE=2                                    !TYPE2: one field winding,one damper winding in
   d-axis,
                                                       !one damper winding in q-axis. Saturation excluded
            SN=4.33 UN=6.6                             !Inertia constant and damping constant
            H=0.370 D=0 !H=2                          !Reactances[p.u] d- axis
            XD=2.36 XDP=0.249 XDB=0.1675               !Reactances[p.u] q- axis
            XQ=2.32 XQB=0.189                          !open circuit subtransient and transient time
            TDOP=1.750 TDOB=0.092 TQOB=0.090

                                                                                    Page 1
```

Figure D.14: *DYNPOW file for DIPLAB case, page 1*

```
DIPLAB_dynpow

constants
!       X0=0.092 X2=0.2827              !Zero sequence reactance and negative sequence
reactance
                XA=0.151 RA=0.0068      !Armature reactance and resistance
                V1D=1.0 V2D=1.2 SE1D=0.1 SE2D=0.3   !Saturation
                VREG=1  !3                  !Voltage regulator identification number  VREG=6
!               TURB=0                  !  TURB=101

!!3 ph generator, salient poles for hydro applications, Gamesa Electrics machine type:SV 100/70/6
!DG3 GEN3 TYPE=2                        !TYPE2: one field winding,one damper winding in
d-axis,
!               SN=4.6 UN=6.6           !one damper winding in q-axis. Saturation excluded
!               H=0.715 D=0 !H=2        !Inertia constant and damping constant
!               XD=1.334 XDP=0.335 XDB=0.273    !Reactances[p.u] d- axis
!               XQ=0.837 XQB=0.422      !Reactances[p.u] q- axis
!               TDOP=2.720 TDOB=0.023 TQOB=0.048    !open circuit subtransient and transient time
constants
!               X0=0.125 X2=0.348       !Zero sequence reactance and negative sequence
reactance
!               XA=0.1 RA=0.00219       !Armature reactance and resistance
!               V1D=1.0 V2D=1.2 SE1D=0.1 SE2D=0.3   !Saturation
!               VREG=7  !4                  !Voltage regulator identification number

!!3 ph generator with cylindrical rotor, Alconza-Berango, S.L Type NIIR5060 A-4LW
DG4 GEN4  TYPE=3                        !TYPE3: Model with one field winding and no damper
windings.
                SN=2.5 UN=0.69          !one damper winding in q-axis. Saturation excluded
                H=1 D=0 !H=2            !Inertia constant and damping constant
                XD=2.656 XDP=0.136 XDB=0.098    !Reactances[p.u] d- axis
                XQ=2.527 XQB=0.105      !Reactances[p.u] q- axis
                TDOP=3.3997             !open circuit transient time constants
                X0=0.125 X2=0.348       !Zero sequence reactance and negative sequence
reactance
                XA=0.1 RA=0.00219       !Armature reactance and resistance
                V1D=1.0 V2D=1.2 SE1D=0.1 SE2D=0.3   !Saturation

                                                Page 2
```

Figure D.15: *DYNPOW file for DIPLAB case, page 2*

```
                                DIPLAB_dynpow
      VREG=2    !5                          !Voltage regulator identification number
END

REGULATORS
!for DG1 and DG3
1 TYPE=DSL/EXCITERAC8B/ E1=2.222 SE1=1.346 E2=2.962 SE2=1.9
                        TE=0.5 KE=1.0 TA=0 VRMIN=0 VRMAX=35 KA=1.0
                        TD=0.01 KD=24 KI=145 KP=150
!for DG4
2 TYPE=DSL/EXCITERAC8B/ E1=2.222 SE1=1.346 E2=2.962 SE2=1.9
                        TE=0.5 KE=1.0 TA=0 VRMIN=0 VRMAX=10 KA=1.0
                        TD=0.01 KD=25 KI=150 KP=160
!Bruvollelva, values from the AVR at Snaasa, Var mode
9 TYPE=DSL/EXCITERSIN/  E1=2.222 SE1=1.346 E2=2.962 SE2=1.9
                        YMIN=-0.1 YMAX=0.1 VMAX=0.1 KII=3.0 VMIN=-0.1  KG=1.0
                        TE=0.5 KE=1.0 TA=0 VRMIN=0 VRMAX=10 KA=1.0
                        TD=0.08 KD=66.3 KI=148.5 KP=177.2
                        NREG=GEN1 GEN11
!Bruvollelva, values from the AVR at Snaasa, PF mode
10 TYPE=DSL/EXCITERQE/  E1=2.222 SE1=1.346 E2=2.962 SE2=1.9
                        YMIN=-1 YMAX=1 VMAX=1 KII=10 VMIN=-1 KG=1
                        TE=0.5 KE=1.0 TA=0 VRMIN=-1 VRMAX=10 KA=1.0
                        TD=0.08 KD=66.3 KI=148.5 KP=177.2
                        NREG=GEN1 GEN11
END

DSL-TYPES
!Automatic voltage regulator (AVR)
 EXCITERAC8B(E1,SE1,E2,SE2,VC,TI/1/,TE,KE,TA,VRMIN,VRMAX,KA,TD,KD,KI,KP,UF,UF0)

 !AVR with VAR control (reactive power)
EXCITERQE(E1,SE1,E2,SE2,VC,QE,YMIN,YMAX,VMAX,KII,TII/1/,VMIN,KG,TI/1/,TE,KE,TA,
          VRMIN,VRMAX,KA,TD,KD,KI,KP,UF,UF0)

                                                                    Page 3
```

Figure D.16: *DYNPOW file for DIPLAB case, page 3*

```
DIPLAB_dynpow
!AVR with sinfi control (power factor control)
EXCITERSIN(E1,SE1,E2,SE2,VC,PE,QE,YMIN,YMAX,VMAX,KII,TII/1/,VMIN,KG,TI/1/,TE,KE,TA,
           VRMIN,VRMAX,KA,TD,KD,KI,KP,UF,UF0)
  END
TURBINES
  101  TYPE 22 TAB 10
END
SHUNT
  DIPLAB 1BREAKER=1 !Xsc
END
BREAKERS
  1 TYPE=0
END
END
```

Figure D.17: *DYNPOW file for DIPLAB case, page 4*

D.4 In-House Lab

```
1 kW Lab
**
GENERAL
 SN=0.001    !snåsa transformer rating
END

NODES
 BUS1  UB=0.400    AREA=1
 BUS2  UB=0.400    AREA=1
 BUS3  UB=0.400    AREA=1
 BUS4  UB=0.400    AREA=1
END

LINES
 BUS1  BUS2  TYPE=0 !Legges ut ved lang kabel
 BUS3  BUS4  TYPE=0                                    !Legger inn en
kortslutning parallelt med Xsr
END

SHUNT IMPEDANCES
 BUS3 X=14.85 1BREAKER=1 NCON=1!X.sc
END

SREACTORS
BUS2 BUS3 TYPE=1 X=14.85 !Xsr
BUS1 BUS2 TYPE=1 R=0.270 X=0.00211 !Legges inn ved lang kabel
END

BREAKERS
 1 TYPE=0
END

TABLES
1 TYPE=2 F= -1  0.02    !Re (rotor resistance) as a function of the slip!
constant, Re=0.02
             1  0.02
END

POWER CONTROL
 BUS1 TYPE=NODE NAME=STIFF RTYP=SW  U=0.400   FI=0
 BUS4 TYPE=NODE NAME=DG1   RTYP=PQ  Q=0  P=0.001099
END
END
```

Figure D.18: *OPTPOW file for in-house lab*

```
Lab machine, 1 kW
**
CONTROL DATA
 TEND=20 !stop simulation (time)  TEND=10   20  150
 SPL=0.05
 TETL=180
 ! DEND=-1 skips presimulation
END

GENERAL
 FN=50    !frequnecy
 REF=BUS1 !infinite bus is used as referance machine
END

NODES
 BUS1 TYPE=1 R=2 X=20
END

SYNCHRONOUS MACHINE
!3 ph generator, salient poles
DG1 BUS4 TYPE=2
d-axis,
        SN=0.001 UN=0.400
excluded
        H=0.0936 D=0
        XD=0.78 XDP=0.30 XDB=0.12
gives an invalid TF
        XQ=0.507 XQP=0.507 XQB=0.1
        TDOP=0.1014 TDOB=0.036 TQ0B=0.036
constants
        XA=0.08 RA=0.066
        SE1=0.05 SE2=0.10
        TURB=0
END

TURBINES
                                                !TYPE2: one field winding,one damper winding in

                                                    !one damper winding in q-axis. Saturation

                                            !Inertia constant and damping constant
                                             !Reactances[p.u] d- axis. Measured: XDB=0.10, but this

                                                    !Reactances[p.u] q- axis
                                            !open circuit subtransient and transient time

                                            !Armature reactance and resistance

                                            !  TURB=101

                                                                                    Page 1
```

Figure D.19: *DYNPOW file for in-house lab, page 1*

```
  101   TYPE 22 TAB 10
  END
SHUNT
  BUS3 1BREAKER=1 !Xsc
END
BREAKERS
  1 TYPE=0
END
RUN INSTRUCTION
  AT 1.000 INST CONNECT SHUNT BUS3
  AT 1.000 INST CLOSE SHUNT BUS3 1BREAKER PHASE 123
! AT 1.000 INST DISCONNECT LINE BUS2 BUS3
  AT 1.078 INST OPEN SHUNT BUS3 1BREAKER PHASE 123
! AT 1.10 INST CONNECT LINE BUS2 BUS3
END
END
```

Figure D.20: *DYNPOW file for in-house lab, page 2*